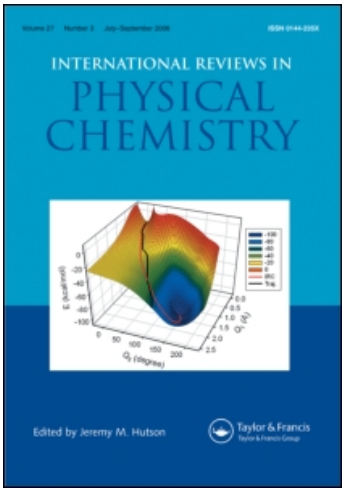

International Reviews in Physical Chemistry
Publication details, including instructions for authors and subscription information:
http://www.informaworld.com/smpp/title~content=t713724383

Nuclear magnetic resonance techniques for the study of mechanisms of diffusion in solids

A. V. Chadwick[a]
[a] University Chemical Laboratory, University of Kent, Canterbury, Kent, U.K.

To cite this Article Chadwick, A. V.(1988) 'Nuclear magnetic resonance techniques for the study of mechanisms of diffusion in solids', International Reviews in Physical Chemistry, 7: 3, 251 — 280
To link to this Article: DOI: 10.1080/01442358809353214
URL: http://dx.doi.org/10.1080/01442358809353214

INTERNATIONAL REVIEWS IN PHYSICAL CHEMISTRY, 1988, VOL. 7, NO. 3, 251–280

Nuclear magnetic resonance techniques for the study of mechanisms of diffusion in solids

by A. V. CHADWICK
University Chemical Laboratory, University of Kent, Canterbury, Kent CT2 7NH, U.K.

The identification of mechanisms of diffusion in solids by NMR methods has been used increasingly in recent years. We demonstrate the role of NMR methods in this general area by the consideration of a few selected examples. Particular attention is given to the work on crystals that have the fluorite structure, as these have been used to test the various available NMR procedures which now provide a sophisticated approach to the study of diffusion mechanisms. Other examples which we consider show how more general information on diffusion can also be obtained by NMR methods.

1. Introduction

The most common application of nuclear magnetic resonance (NMR) spectroscopy in chemistry is to probe molecular structure via the local magnetic environment of the nuclei. The equipment is usually a commercially manufactured high-resolution spectrometer and the sample is in the liquid phase. Modern spectrometers with high-field magnets, Fourier transform facilities and computer-averaging techniques make possible the study of detailed chemical structure in hitherto difficult systems, i.e. nuclei with small magnetic moments (e.g. ^{107}Ag and ^{109}Ag) or dilute spin systems (e.g. ^{13}C), and NMR spectroscopy is now an indispensable tool for the organic and inorganic research chemist (see, for example, Akitt (1982) and Harris (1983)). The recent advent (Andrew 1981, Lippmaa *et al.* 1981) of cross-polarization and magic-angle spinning has further widened the scope of NMR and allows high-resolution spectra to be recorded for solid samples. An important example of this development is the key role that ^{29}Si and ^{27}Al NMR now play in the investigation of zeolite structures (Fyfe *et al.* 1983, Klinowski 1984, Thomas and Klinowski 1985). In addition to providing structural information NMR is a powerful probe of molecular motion and it is this facet of NMR that has a long-standing role in physics and physical chemistry. For this application the spectrometers are often home-built or modified commercial equipment and are often specially designed for a particular type of experiment. NMR techniques have been highly successful in providing information on reorientational and translational motion in a wide range of materials, including liquids (Powles 1959, Noack 1971), solids (Ailion 1971, Allen 1972) and liquid crystals (Luckhurst and Gray 1979). This information can be of a general nature (e.g. detecting phase transitions, identifying mobile species, estimating activation energies, etc.) or very specific (e.g. providing accurate diffusion coefficients, yielding the anisotropy of motions, etc.). It is the specific application of NMR techniques in the study of the mechanisms of translational diffusion in solids that is treated in this article. This has been an area of growing interest and steady progress has been achieved over the last twenty years, often involving the combination of NMR with other techniques, with significant developments in both theory and experimentation. The general aims are to review some of these developments, to show

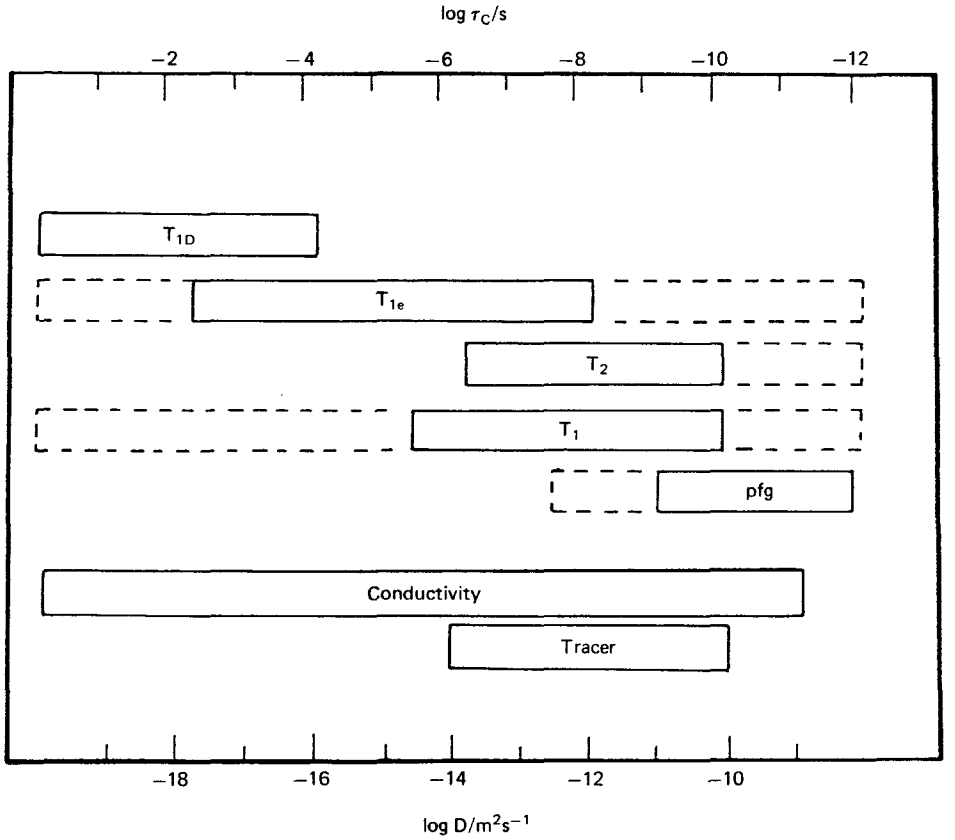

Figure 1. The range of diffusion coefficients that can be studied in solids using NMR methods. The boxes with full lines indicate the specific case where the techniques have been employed to study F^- ion diffusion in crystals with the fluorite structure (Gordon and Strange 1979). Boxes in dashed lines indicate the limits that could be available in other systems.

the principles involved in the studies, to outline the methods of data interpretation and to indicate the potential of currently available methods from the viewpoint of an experimental solid state chemist. A detailed discussion of the NMR experiments and theory is not given (but see Slichter (1973) and Harris (1983)). Much of the work discussed is taken from the research of the author.

There are a variety of NMR methods which, taken together, can be regarded as an excellent general tool for the investigation of self-diffusion in solids. An outstanding feature is the enormous range of self-diffusion coefficients, from 10^{-16} to 10^{-4} cm^2 s^{-1}, that can be explored by NMR methods. The limits of individual methods are indicated in figure 1. In comparison to the conventional radiotracer diffusion techniques (Shewmon 1963, Adda and Philibert 1966), NMR methods have the advantages of being rapid and non-destructive. There are no major restrictions on the types of material that can be studied by NMR—molecular, ionic and metallic solids all being amenable, and the samples can be amorphous, single crystals or powders. Although the majority

of diffusion studies have been concerned with the more easily accessible nuclei (e.g. ^{1}H, ^{7}Li, ^{19}F, ^{23}Na) it should be possible, with the advent of modern equipment (e.g. high-field magnets, multi-nuclear probes etc.) to study diffusion of materials containing one or more of a large number of other elements in the Periodic Table. An advantage of NMR over some types of diffusion experiment, for example those employing measurement of conductivity and creep, in multi-component systems is that the mobile species is readily identified and it is often possible by distinguish between local and long-range motion. However, despite these numerous advantages, there are some limitations, disadvantages and pitfalls with NMR methods. One limitation is that NMR experiments do not have the sensitivity of the radiotracer methods and could not be used to study impurity diffusion in dilute systems. It is also difficult to study diffusion by NMR methods in paramagnetic systems; it is just about manageable using low magnetic fields. A related pitfall is that in some systems, as will be explained later, the presence of traces of paramagnetic impurities at p.p.m. levels can give misleading results by masking the true effects of diffusion. A major problem with the bulk of the NMR methods is the difficulty in translating the raw experimental data (e.g. spectral line-widths or relaxation times) into diffusion coefficients. In essence, this is due to the difficulty in obtaining an adequate theoretical model which can relate the microscopic motions of an ensemble of magnetic spins to a macrosopic diffusion coefficient of atoms. If only an order of magnitude estimate of the diffusion coefficient is required or if a screening of a group of materials for relative diffusion parameters is to be undertaken then simple models are available which can be used for such purposes. However, more sophisticated models are necessary if accurate diffusion coefficients are required. These models have only recently become available and are still restricted to systems with relatively simple crystal structures.

From the considerations outlined above the examples given here of the role NMR can play in the investigation of diffusion mechanisms are necessarily restricted to materials of rather simple structures. The identification of diffusion mechanisms in solids is no mean task, irrespective of the technique employed, and has been successfully achieved only in materials with simple structures. Some of the work quoted here is intentionally devoted to model materials to test the viability of the techniques. The examples will reflect the current state of the art, show the potential of these NMR methods and point to future developments.

These examples cover the various approaches that have been employed to use NMR methods in mechanistic studies of diffusion. They include methods:

(*a*) which rely solely on NMR measurements of diffusion i.e. the dependence of diffusion on a thermodynamic variable (e.g. temperature T or pressure P);
(*b*) where essentially structural information from NMR studies is employed to gain an insight into diffusion processes; and
(*c*) which combine NMR diffusion measurements with diffusion data obtained via other techniques.

The last method is very powerful but does rely on accurate diffusion data from both sources. Examples have been taken from studies of molecular and ionic crystals. Both these classes of material contain systems with easily accessible NMR nuclei (for the molecular crystals ^{1}H, ^{19}F, ^{31}P and for ionic crystals ^{19}F, ^{7}Li, ^{23}Na and ^{205}Tl) and, equally important, can be prepared as well-characterized samples. The NMR diffusion studies in molecular crystals have been reviewed (Chezeau and Strange 1979) and here some of the work on the so-called 'plastic crystals' will be discussed. In this group of

materials the molecules are globular, undergo endospherical reorientation, form cubic or hexagonal structures and exhibit relatively rapid diffusion (Sherwood 1979 a) and have been widely studied by NMR methods (Boden 1979). NMR methods have been used to study 'normal' ionic crystals and the data were reviewed by Corish and Jacobs (1973) over a decade ago. However, it is for the materials referred to as 'fast-ion conductors' (sometimes referred to as 'solid electrolytes' or 'superionic conductors') that NMR methods are proving particularly fruitful (Whittingham and Silbernagel 1977, Richards 1979, Brinkmann 1983). Here, the ionic conductivity is unusually high, comparable to a molten salt, and the interest lies in the potential applications in devices, particularly in solid state batteries. The fluorides with the fluorite structure exhibit both normal and fast-ion conductivity, depending on the temperature regime, and provide excellent examples of NMR studies of diffusion processes.

2. The basic principles of the NMR experiments

The basic theories and techniques of NMR can be found in standard texts (Abragam 1961, Goldman 1970, Slichter 1973) and the pulsed experiments have been the subject of books (Farrar and Becker 1971, Harris 1983). The object here is to recall the principles and then to indicate how the measured parameters are related to diffusion coefficients.

2.1. *Line-width experiments*

Consider a simple NMR experiment involving a solid containing nuclei with spin I equal to $\frac{1}{2}$ (^{1}H or ^{19}F) and magnetic moment μ. The magnetogyric ratio γ is defined as μ/p, where p is the nuclear angular momentum $I\hbar$, and is characteristic for each magnetic isotope. When a sample of the solid is placed in the field $\mathbf{B}_0$ of the spectrometer magnet there are two quantum levels, the Zeeman levels, for the spins, parallel and anti-parallel to $\mathbf{B}_0$, and the energy separation between these states is $\gamma\hbar B_0$. In a continuous-wave (c.w.) experiment the sample is subjected to an oscillating magnetic field $\mathbf{B}_1$, applied perpendicular to the $\mathbf{B}_0$ field. As the frequency ω of the $\mathbf{B}_1$ field is swept, absorption will occur at the resonance condition $\hbar\omega_0 = \gamma\hbar B_0$, and there will be excitation from the lower to upper spin states. This resonance frequency is the Larmor precession frequency ω_0, equal to γB_0. For practical magnets the values of γ define ω_0 in the radiofrequency (r.f.) region of the electromagnetic spectrum. In a liquid the absorption line will be sharp, provided the magnetic field $\mathbf{B}_0$ is homogeneous. This simple experiment is shown schematically in figure 2 (*a*).

In a rigid solid, i.e. where there is no relative motion of the atoms, the absorption line is not sharp. This is because the randomly aligned nuclear magnetic dipoles create magnetic fields which add vectorially to $\mathbf{B}_0$. Thus the effective (local) magnetic field $\mathbf{B}_{\text{eff}}$ will be the sum of $\mathbf{B}_0$ and the local field $\mathbf{B}_{\text{local}}$, and will vary from site to site within the lattice, giving a distribution of resonance frequencies and a finite line-width $\Delta\omega$. The effects are shown schematically in figure 2 (*b*). The effect of isotropic diffusional motion will be to average out the local fields and cause the line to narrow. Thus the diffusion coefficient D is proportional to $1/\Delta\omega$ and line-width measurements from c.w. experiments can be used to estimate D. For diffusion involving a single mechanism D will follow a simple Arrhenius behaviour, i.e.

$$D = D_0 \exp(-Q^*/kT), \tag{1}$$

where D_0 is the pre-exponential factor and Q^* is the activation energy. Thus relatively accurate values of Q^* can be obtained from line-width measurements by plotting

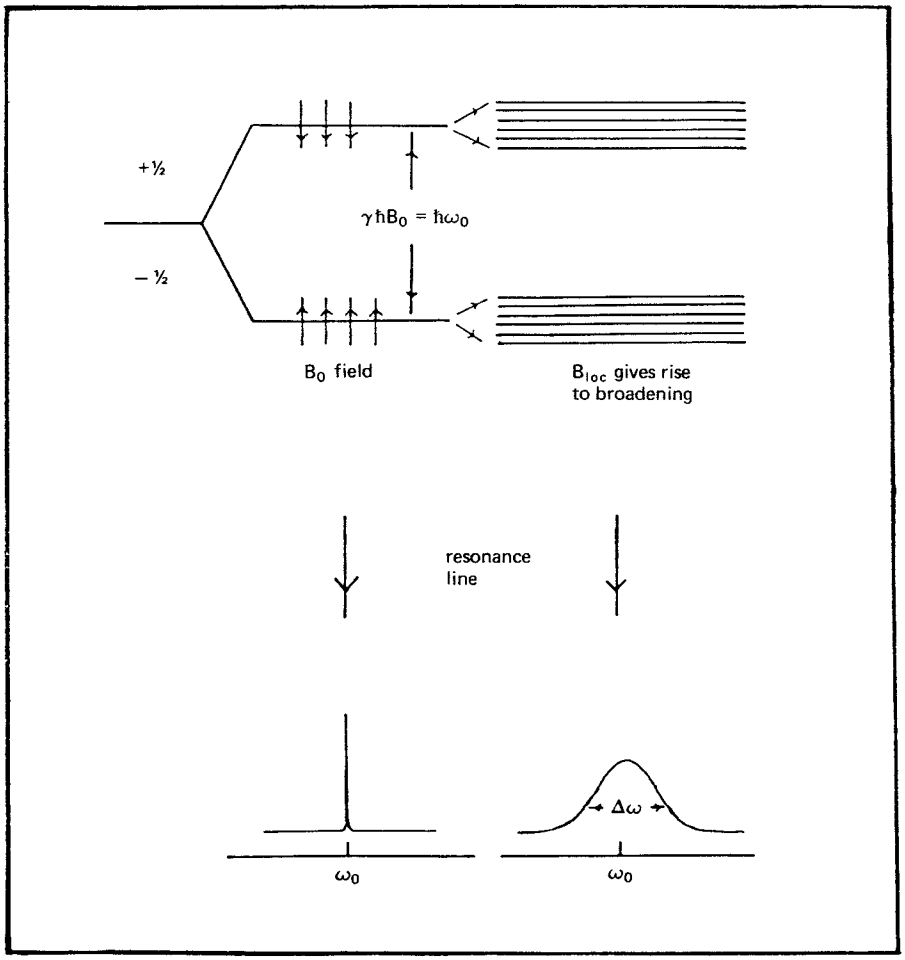

Figure 2. A schematic representation of the continuous wave (c.w.) experiment for a spin $\frac{1}{2}$ nucleus. In liquids a sharp, narrow absorption line is seen at the Larmor frequency ω_0 (on the left). In a solid the local dipolar fields from neighbouring nuclei split the quantum levels and the absorption line is still centred on ω_0 but broadened (on the right).

$\log(\Delta\omega)$ versus $1/T$. Usually the experiment would be performed on a broad-line spectrometer. However, for organic plastic crystals, the lines are sufficiently narrow to be observed on a high-resolution instrument, i.e. $\Delta\omega < 1$ kHz (Boden 1979), but care must be taken to ensure that inhomogenous broadening does not inadvertently occur due either to the magnet or to the susceptibility and shape of the sample (Chadwick *et al.* 1976).

2.2. *Relaxation time measurements*

The basis of most of the modern NMR measurements is the use of pulsed experiments (Farrar and Becker 1971, Akitt 1982, Harris 1983), i.e. subjecting the sample to short bursts of pulses of high intensity r.f. power and following the resulting time dependence of the magnetization of the sample along particular directions. The

pulse can be varied in terms of frequency, angle with respect to the $\mathbf{B}_0$ field, phase and length (duration of the pulse) and often the experiments involve a complex sequence of pulses. The effect of these pulses is best visualized in terms of a classical picture of the motion of spinning magnets of moment μ in an applied magnetic field. Thus a single spinning magnet precesses around the applied $\mathbf{B}_0$ field with frequency ω_0 and describes a cone at an angle θ to the $\mathbf{B}_0$ field. For an assembly of magnets they can be regarded as spread evenly over this cone giving a net, small magnetization along the $\mathbf{B}_0$ direction but no magnetization perpendicular to the $\mathbf{B}_0$ direction. The effect of pulsed r.f. power applied at frequency ω_0 and perpendicular to the $\mathbf{B}_0$ field is to tip the precession cone and change the direction of the magnetization.

A basic pulse experiment is to apply an intense $\mathbf{B}_1$ field at resonance to tip the magnetization by 90° to the $\mathbf{B}_0$ direction, usually defined as the z direction. Thus there will be an observable oscillating magnetization in the x or y direction. However, since there is a spread of Larmor frequencies in a solid this magnetization will decay as the precessing spins dephase. This is termed the free induction decay (FID) which is the Fourier transform of the c.w. signal. The time constant for this decay (i.e. the time for the magnetization in the transverse direction to fall to $1/e$ of its original value) is termed the transverse or spin–spin relaxation time T_2, and is approximately equal to $1/\Delta\omega$. In terms of the thermodynamics of the system T_2 is the relaxation time for the spins to come to an internal equilibrium following a perturbation.

In the above experiment after a sufficient time the spins will return to a precession about the $\mathbf{B}_0$ field and the original magnetization along the z direction will be recovered. The characteristic relaxation time for this process is termed the longitudinal or spin–lattice relaxation time T_1. For this relaxation the spins must exchange energy with the surrounding lattice and it will be a resonance process involving quanta equal to the energy separation between the Zeeman levels.

There are two other relaxation times that can be measured in pulse experiments and are used in diffusion studies. These involve the use of pulse sequences which can 'lock' the spins along certain directions and effectively remove the $\mathbf{B}_0$ field. Thus spin–lattice relaxation processes can be studied in much smaller fields than $\mathbf{B}_0$. The first of these times is the spin–lattice relaxation time in the rotating frame, $T_{1\rho}$, where spin–lattice relaxation in the $\mathbf{B}_1$ field is observed. Since $\mathbf{B}_1$ is $\sim 10^{-3} \times \mathbf{B}_0$ the smaller separation of the Zeeman levels, $\gamma\hbar\mathbf{B}_1$, means that smaller quanta are required to cause relaxation. Relaxation in the local dipolar field $\mathbf{B}_{\text{local}}$ is characterized by the relaxation time T_{1D} and, since $\mathbf{B}_{\text{local}} < \mathbf{B}_1 < \mathbf{B}_0$, involves even smaller quanta.

2.3. *Relation between relaxation times and diffusion coefficients*

Let us now consider what are the effects of molecular motion on the relaxation times in a simple system where only the interactions between the magnetic dipoles are important (i.e. quadrupolar and paramagnetic interactions are neglected). The thermal motion of a single nuclear magnetic dipole by a series of random diffusive jumps will create an oscillating magnetic field. This will be like a 'noise spectrum' and will contain components at all frequencies. Components of this spectrum will correspond to the separation between the spin levels and these will cause relaxation by stimulated emission. Therefore, in order to determine the relaxation rate the intensity dependence on frequency of the oscillating field, the spectral density $J(\omega)$, has to be known. Qualitatively, the spectral density will spread out as the temperature is increased, and this is shown schematically in figure 3. If we remain with the qualitative picture then the effect of temperature on T_1 can be very informative.

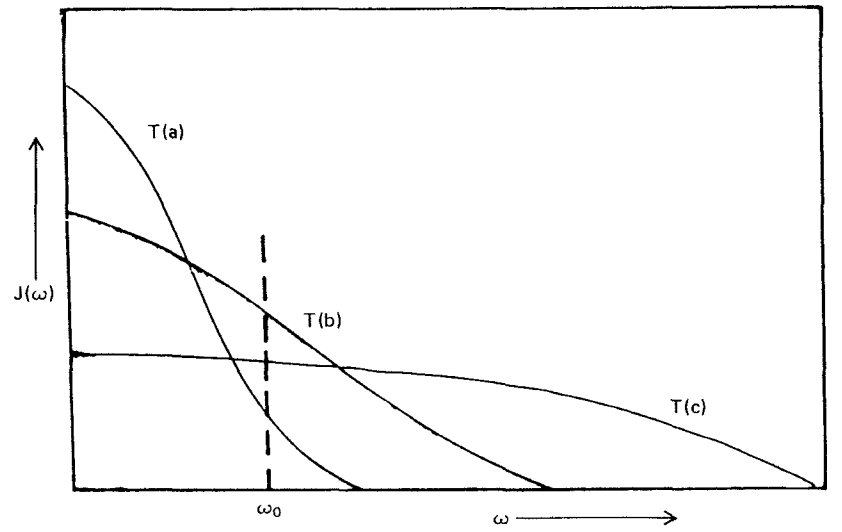

Figure 3. A schematic representation of the spectral density, i.e. the intensity of the fluctuating magnetic field due to motion of the nuclei, as a function of frequency. The curves 'spread' out with increasing temperature ($T(c) > T(b) > T(a)$), the intensity at ω_0 first increasing the then decreasing.

T_1 will be affected by the components of the spectral density at the Larmor frequency, ω_0. At low temperatures the diffusion is slow and the intensity at ω_0 will be small, hence T_1 will be long. As the temperature increases the motion speeds up, the intensity of components at ω_0 increase, and T_1 decreases. However, a stage will be reached where the effect of spreading of the spectral density will start to reduce the intensity at ω_0 and T_1 will start to increase. Thus T_1 will show a minimum in its temperature dependence, as indicated schematically in figure 4. In a similar manner the temperature dependence of the other relaxation times can be rationalized. T_2 is dominated by components at $\omega = 0$, $T_{1\rho}$ by components at the Larmor frequency in the $\mathbf{B}_1$ field, ω_1, and T_{1D} by components at the Larmor frequency in the $\mathbf{B}_{local}$ field, ω_D. Thus qualitatively it can be seen that moving from T_1 to $T_{1\rho}$ to T_{1D} there is an increase in the sensitivity to the slower motions.

The precise relationship between diffusion and the relaxation times requires a model to relate the molecular motion of the assembly of magnetic dipoles to the spectral density. The difficulty lies in obtaining a physically realistic model. The earliest model, due to Bloembergen, Purcell and Pound (1948), referred to as the BPP model, which was later revised and generalized (Kubo and Tomita 1954, Look and Lowe 1966) assumes an exponential time correlation function $G(\tau)$. This is defined in terms of the correlation of the local field at time t, $\mathbf{B}(t)$, with this field at a time τ later, $\mathbf{B}(t+\tau)$ and can be written as

$$\overline{\langle \mathbf{B}(t) \cdot \mathbf{B}(t+\tau) \rangle} = G(\tau)\, B(0)^2$$

where the average is taken over time and over the ensemble of spins. This describes the persistence of the fluctuations in the oscillating field caused by diffusive motion, and the assumption of an exponential correlation function gives

$$G(\tau) = G(\tau = 0) \exp(-|\tau|/\tau_c) \qquad (2)$$

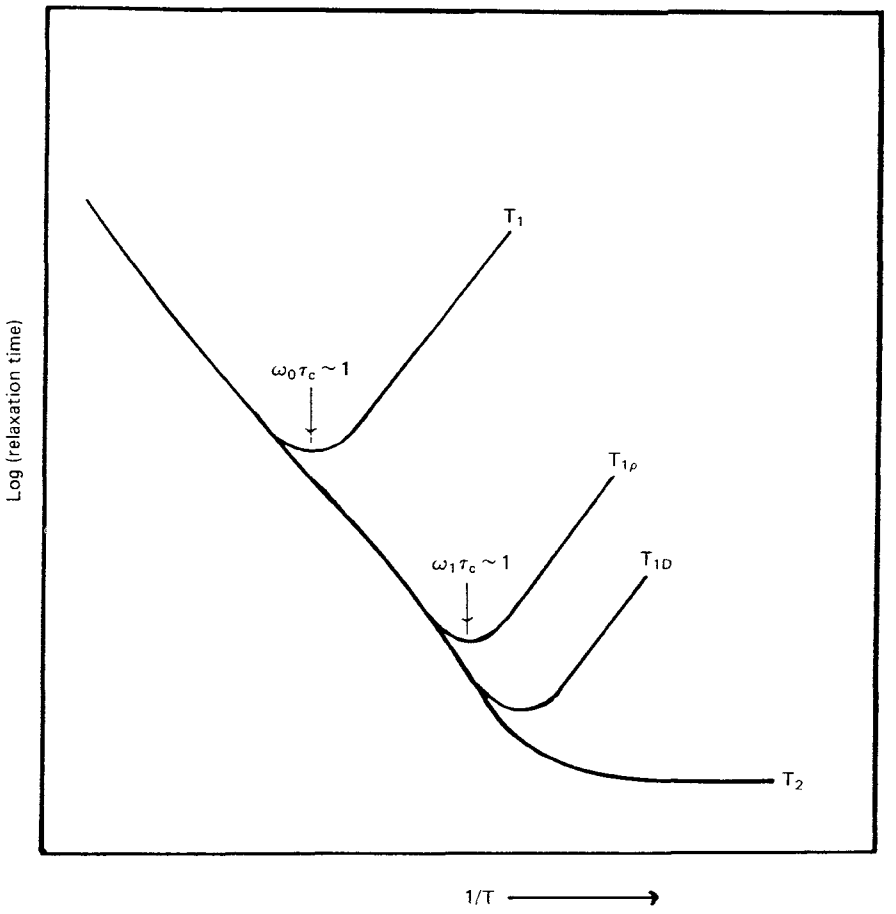

Figure 4. A schematic representation of the temperature dependence of the relaxation times.

where τ is time and τ_c is the correlation time. For translation diffusion τ_c may be interpreted in terms of the mean residence time of an atom on a lattice site. This allows expressions for the relaxation times to be developed. These can be formulated precisely. However, here only the general results are required, and these are of the form

$$\frac{1}{T_1} \propto \frac{\tau_c}{1+\omega_0^2\tau_c^2}, \tag{3}$$

$$\frac{1}{T_{1\rho}} \propto \frac{\tau_c}{1+4\omega_1^2\tau_c^2} \quad \text{when } \omega_0\tau_c \gg 1, \quad \text{and } \frac{1}{T_{1\rho}} = \frac{1}{T_1} \quad \text{when } \omega_0\tau_c \ll 1 \tag{4}$$

$$\frac{1}{T_2} \propto \tau_c \quad \text{provided } \gamma \mathbf{B}_{\text{local}}\, \tau_c \ll 1. \tag{5}$$

Once the value of τ_c has been determined then the diffusion coefficient is evaluated from the Einstein equation (Adda and Philibert 1966)

$$D = \frac{a^2}{6\tau_c} \tag{6}$$

where a is the jump distance. Combining equation (1) with equation (6) leads to

$$\tau_c = \tau_c^0 \exp Q^*/kT \tag{7}$$

and the resulting temperature dependence of the relaxation times is shown in figure 4. It is interesting to note the importance of the minima in T_1 and $T_{1\rho}$ as these provide good estimates of τ_c, i.e. at the T_1 minimum $\tau_c \approx 1/\omega_0$ and at the $T_{1\rho}$ minimum $\tau_c \approx 1/\omega_1$. Experimental data are much easier to interpret if these minima are observed.

The BPP model was developed to treat molecular motion in liquids and the spectral density used is not appropriate to diffusion in crystalline solids. Calculations of the spectral densities for a solid were carried out by Torrey (1953, 1954) and Resing and Torrey (1963). The model assumed that the magnetic dipoles perform a random walk on an 'isotropic' lattice by allowing jumps to any point on the surface of a sphere with a radius equal to the nearest-neighbour distance. This is a reasonable approximation for polycrystalline samples of b.c.c. and f.c.c. materials (Scholl 1974, 1975). However, the model ignores the correlation between successive jumps which would be expected in diffusion mechanisms involving point defects. In addition, the model, since it assumes isotropic diffusion, is applicable only to polycrystalline samples. The anisotropy or relaxation times was first treated by Eisenstadt and Redfield (1963). In their model a random walk treatment was used for atomic jumps between lattice sites and then an estimate was made to correct for correlation effects. This model is referred to as the 'encounter model' as it considers the effect of a defect moving into the vicinity of a nucleus, the encounter, and the sequence of jumps that will result.

In NMR it is necessary to consider two contributions to the correlation effect in point-defect-assisted diffusion. The first is the *spatial* part which arises because not all encounters of a nucleus result in a net displacement of the nucleus. This effect is well-known for radiotracer diffusion and will be mentioned later. The second part is *temporal* and arises because jumps within an encounter are too fast to cause relaxation and many encounters are required to cause appreciable relaxation. Recently Wolf (1974 a, b, 1975 a, b, 1979) has developed the encounter model to give a thorough treatment of correlation effects for defect diffusion in polycrystalline and single crystals samples of b.c.c. and f.c.c. materials. Thus accurate diffusion coefficients can be evaluated from the relaxation times and the sample orientation dependence of the relaxation time predicted for single crystals. This was a crucial development in mechanistic studies.

2.4. *Pulsed field gradient NMR*

The pulsed field gradient (p.f.g.) NMR technique has been used mainly to study self-diffusion in liquids (Stejskal and Tanner 1965, Gross and Kosfield 1969). In this experiment the nuclear spin state is used as a label for the atoms and the effect of translational diffusion on the spin-echo amplitude allows a direct measurement of the self-diffusion coefficient. Unlike the situation for relaxation time measurements, the time-scale of the experiment is long and therefore the atoms undergo very many diffusive jumps and will traverse relatively long distances. The results obtained in this way are, therefore, comparable to those obtained in radiotracer studies. The technique can be applied to relatively fast diffusion in solids, $D > 10^{-9}\,\mathrm{cm^2\,s^{-1}}$, and an apparatus has been described (Gordon *et al.* 1978) which is capable of these measurements at temperatures up to 1300 K. One advantage of p.f.g. measurements is that they are less susceptible to interference from paramagnetic impurities than relaxation time

measurements. It should be noted that D from p.f.g. measurements is equivalent to the radiotracer diffusion coefficient.

3. Strategies used to identify diffusion mechanisms

Except for the anomaly of grain-boundary migration, in a crystalline solid the diffusion occurs via the point defects, the simplest being the vacancy and the interstitial atom. Thus the operative mechanisms are:

(*a*) the vacancy mechanism—the exchange of an atom with a vacancy on an adjacent lattice site;
(*b*) the intersitial mechanisms—the migration of the interstitial from interstitial site to interstitial site through the lattice;
(*c*) the interstitialcy mechanisms—the migration of an interstitial onto a normal site with the simultaneous movement of normal atom onto an interstitial site (the motion of the two atoms may be collinear or non-collinear).

It is also possible that two atoms on adjacent sites may change position. This is termed the direct exchange mechanism, and does not involve defects. These four mechanisms are illustrated for the anion sub-lattice of CaF_2 in figure 5. We will now consider in general terms how NMR methods could be used to identify which mechanism might be operative in a particular system.

3.1. *The effect of temperature or pressure on diffusion*

In a pure, one-component solid, the self-diffusion coefficient can be written as (Howard and Lidiard 1964)

$$D=\gamma a^2 v \exp\{-(g_f+g_m)/kT\} \tag{8}$$

Here γ is a geometric factor (depending on the lattice structure), a is the jump distance, v is the lattice vibrational frequency, g_f ($\equiv h_f - Ts_f$) is the free energy of defect formation and g_m ($\equiv h_m - Ts_m$) is the free energy of defect migration. Thus the temperature dependence of D yields the observed activation energy Q^*, equal to $(h_f + h_m)$. The pressure dependence is given by

$$\left(\frac{\partial(\ln D)}{\partial P}\right)_T = \left(\frac{\partial(\ln \gamma a^2 v)}{\partial P}\right)_T - \frac{(v_f + v_m)}{kT}, \tag{9}$$

where $v_f + v_m$ are volumes of defect migration and formation. Since the first term on the right-hand side of equation (9) is usually negligible the observed pressure dependence V^* is equal to $(v_f + v_m)$. Absolute magnitudes of D are not required to extract Q^* or V^*. Thus NMR methods provide a good experimental route to these parameters.

Information on the operative mechanism is obtained by using theoretical calculations to predict Q^* or V^* for the various possible mechanisms. Clearly, the reliability of this approach rests on the calculations. However, for some systems like ionic crystals these are at a very sophisticated level of development for Q^* (Catlow and Mackrodt 1982).

3.2. *Determination of the correlation factor*

This approach was originally used for ionic crystals and combined the results of radiotracer and ionic conductivity measurements (Corish and Jacobs 1973). However, it is possible to replace the radiotracer experiment by NMR methods.

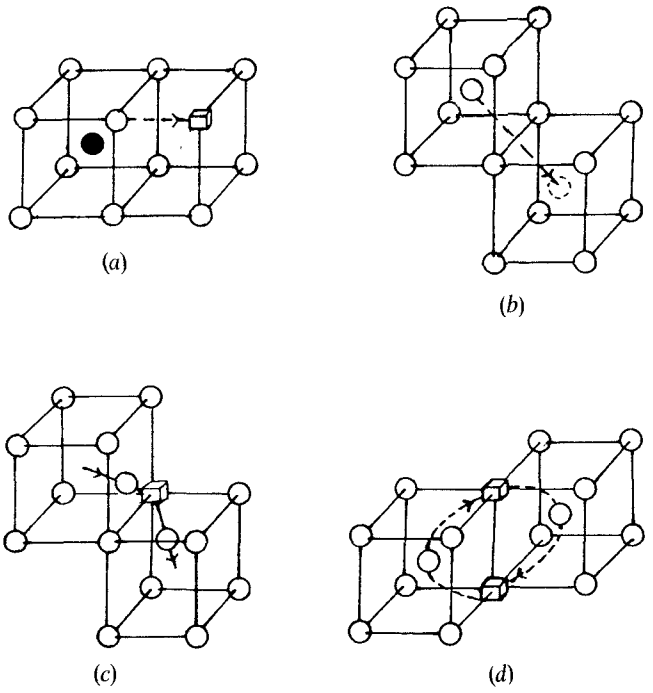

Figure 5. The four possible mechanisms for F^- ion diffusion in CaF_2 (●, cation; ○, anion; □, vacancy). (*a*) Vacancy mechanism, (*b*) interstitialcy mechanism, (*c*) non-collinear interstitialcy mechanism, (*d*) direct exchange. (The collinear interstitialcy mechanism is not allowed as the "in-line" site is occupied by a cation.)

In the measurement of diffusion the motion of labelled atoms, radiotracers or nuclear spin is monitored, and this motion, depending on the operative mechanism, may be correlated, i.e. successive jumps of the atom may not be random. For the radiotracer this is a spatial correlation and is best visualized for a vacancy mechanism. If a labelled atom exchanges places with a vacancy the next most likely jump of the atom is to return to its original site as there is a vacancy on that site. Thus after a given number of jumps of the atom its displacement will be less than it would have been if the jumps had been random. Therefore we can write the tracer diffusion coefficient as

$$D_{\text{tracer}} = f_{\text{tracer}}\, D_{\text{random}}, \tag{10}$$

where D_{random} is the diffusion coefficient for random jumps and f_{tracer} is the correlation factor. Values of f_{tracer} can be accurately calculated for the different mechanisms outlined above (see figure 5) (Compaan and Haven 1958, LeClaire, 1970). The motion of the defect is truly random and the ionic conductivity σ is due to the motion of the defects. The Nernst–Einstein equation (Corish and Jacobs 1973) can be used to calculate a diffusion coefficient from the ionic conductivity D_σ, i.e.

$$D_\sigma = \frac{kT\sigma}{Nq^2}, \tag{11}$$

where q is the effective charge of the defect and N is the number of molecules per unit volume. We can equate D_σ with D_{random} and therefore evaluate f_{tracer} from

$$f_{\text{tracer}} = \frac{D_{\text{tracer}}}{D_\sigma}, \tag{12}$$

compare this with the calculated values, and hence identify the mechanism. The situation, in reality, is not quite so simple as there may be more than one operative mechanism, or a particular mechanism may contribute to D_{tracer} and not D_σ (Corish and Jacobs 1973). In the more recent literature the ratio $D_{\text{tracer}}/D_\sigma$ is termed the Haven ratio, H_{R}.

Clearly, the same approach can be adopted for the combination of NMR relaxation time and measurements of ionic conductivity. Thus a new Haven ratio can be defined as

$$H'_{\text{R}} = \frac{D'_{\text{NMR}}}{D_\sigma}, \tag{13}$$

where D'_{NMR} the diffusion coefficient calculated from the NMR measurements using a model which *neglects* correlation effects. If only one mechanism were operative then the NMR correlation factor f_{NMR}, which includes the temporal and spatial parts, would be equal to H'_{R}. However, the recent development of the Wolf model, referred to in section 2, includes the correlation effects in the analysis of the NMR relaxation times and therefore the diffusion coefficient from such an analysis will be designated D_{NMR}. Thus for the appropriate mechanism of diffusion D_{NMR} will be equal to D_σ.

The importance of combining NMR and conductivity measurements as a mechanistic probe was demonstrated by Hoodless *et al.* (1971, 1973) in NaI and KF. However, it was later work on fluorites that was able to take full advantage of the theoretical developments. This will be discussed in section 4.2.

As a final point in this section it should be noted that neither f_{tracer} nor f_{NMR} is *very* different from unity. For example, for vacancy diffusion in f.c.c. lattices $f_{\text{tracer}} = 0{\cdot}78$ and $f_{\text{NMR}} = 0{\cdot}69$ (for a T_2 experiment), and so a high accuracy in both NMR and conductivity measurements is required. This means that ideally both measurements should be performed on the same samples.

3.3. *Orientation dependence of relaxation times in single crystals*

In single crystals $T_{1\rho}$ depends strongly on the orientation of the crystal axes with respect to the direction of the field $\mathbf{B}_0$ and also depends on the diffusion mechanism (Ailion and Ho 1968). Wolf *et al.* (1977) have given a comprehensive analysis of this effect, and the diffusion induced anisotropies of T_1 and T_2, using the encounter model to treat correlation effects. Although the analysis predicts different anisotropies for different diffusion mechanisms these differences are small compared to the available experimental precision. Thus this elegant approach has yet to find successful application.

In addition to the three specific strategies outlined above it is also possible that NMR methods may yield more general information which can be useful in mechanistic studies. For example, a measured relaxation time may show two components suggesting that two mechanisms are operative. In other situations the structural information from an NMR study may help identify the sites on which the diffusion is occurring when the atoms occupy a number of inequivalent sites.

4. Examples of NMR studies of diffusion mechanisms

4.1. *Plastic crystals*

Molecular crystals in which the molecules are approximately globular (e.g. CH_4, CCl_4, adamantane) undergo a phase transition prior to melting and enter what is termed the plastic, or orientationally-disordered phase (Sherwood 1979 a). In this phase the molecules undergo rapid, endospherical reorientation, form a cubic or hexagonal structure and exhibit relatively high translational mobility (in some cases the crystals will undergo plastic flow under gravity, hence their designation). This feature has attracted considerable attention and several mechanisms of diffusion have been proposed to explain the high mobility of plastic crystals. Since many of these systems are organic solids containing protons NMR has been extensively used in the investigations of diffusion. We shall focus here on one of these materials, hexamethylethane ($(CH_3)_3C.C(CH_3)_3$) which has a b.c.c. plastic phase, and thereby demonstrate the value of NMR measurements.

There have been a number of NMR studies of hexamethylethane (Chezeau *et al.* 1971, Albert *et al.* 1972, Ross and Strange 1978, Britcher and Strange 1979), and the proton T_1 and $T_1\rho$ data of Chezeau *et al.* (1971) for polycrystalline samples are shown in figure 6. The effects in the low temperature phase are due to molecular reorientation and are not of interest here. The effect of self-diffusion on T_1 can be seen just below the melting point where T_1 starts to decrease rapidly. Self-diffusion is more evident in the $T_1\rho$ data where there is a clearly defined minimum. The analyses of the $T_1\rho$, T_2 and line-width data for hexamethylethane using the Wolf model (Britcher and Strange 1979) produces the diffusion coefficients used to construct the Arrhenius plot shown in figure 7. Fitting these data to a single Arrhenius law yielded $Q^* = 68{\cdot}4 \pm 0{\cdot}4\,\mathrm{kJ\,mol^{-1}}$ and, in contrast, the analysis of using a Torrey lattice diffusion model yielded $Q^* = 81{\cdot}3 \pm 0{\cdot}6\,\mathrm{kJ\,mol^{-1}}$. The radiotracer data (figure 7) show clear evidence of curvature (Lockhart and Sherwood 1972) with a higher apparent activation energy at the higher temperatures. The value of Q^* from all the radiotracer points is $86\,\mathrm{kJ\,mol^{-1}}$. Curvature in the NMR diffusion coefficients is less obvious.

Since the plastic crystals have close-packed structures the dominant point defects are expected to be monovacancies which are responsible for the self-diffusion. Simple theoretical estimates (Jost 1960, Sherwood 1973, Chadwick and Glyde 1977) for h_f and h_m for molecular solids lead to the prediction that

$$h_f \cong h_m \cong \text{latent heat of sublimation, } L_s. \tag{14}$$

Thus the predicted value of Q^* is $2L_s$. For hexamethylethane L_s is $39\,\mathrm{kJ\,mol^{-1}}$ therefore the NMR data, yielding $Q^*/L_s = 1{\cdot}7$, provide very strong evidence for the monovacancy being operative. The curvature in the Arrhenius plot for the radiotracer data would suggest another mechanism is also contributing at temperatures close to the melting point. By analogy with metals (Mehrer and Seeger 1972) this other mechanism is probably diffusion via divacancies.

The effect of pressure on the proton T_1 and $T_1\rho$ for hexamethylethane was determined by Ross and Strange (1978) and the results analysed with the Torrey model. Their data, $\log \tau_c$ versus P, are shown in figure 8 for several temperatures. At low temperatures the plots were found to be linear, but at the higher temperatures there are clearly two linear regions. Except for the extreme low pressure, high temperature region, the apparent activation volume V^* is $154 \pm 7\,\mathrm{cm^3\,mol^{-1}}$.

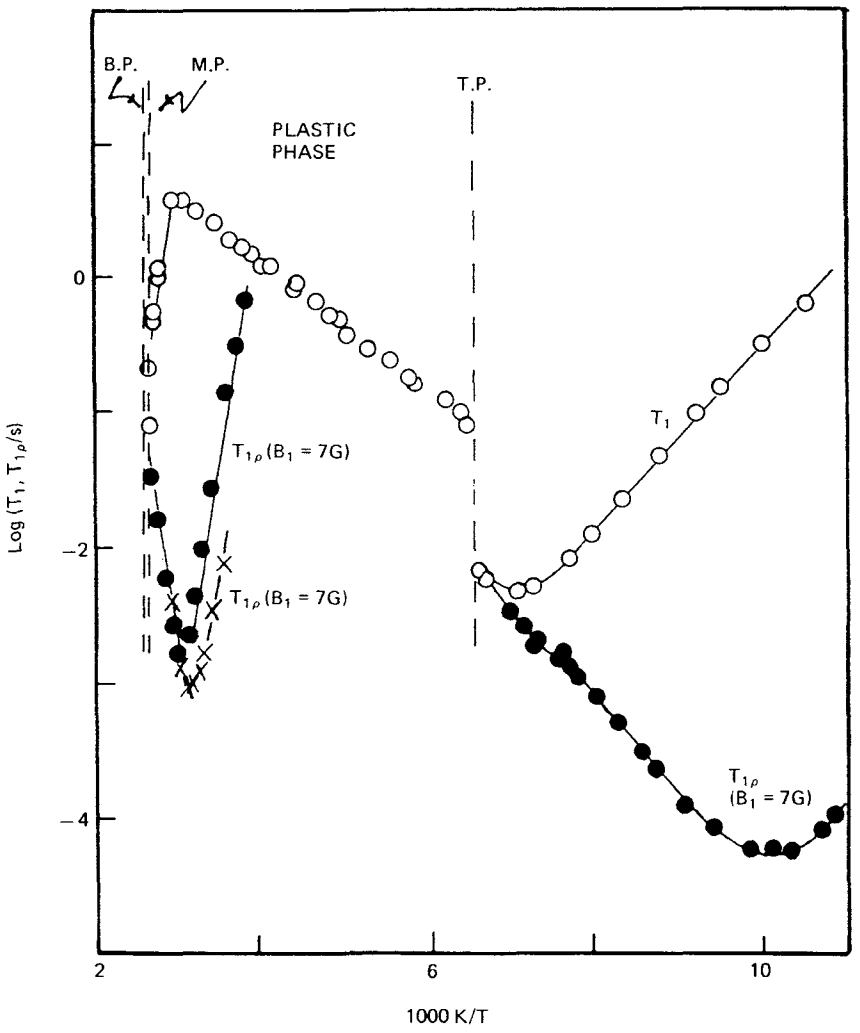

Figure 6. The proton relaxation times as a function of reciprocal temperature for polycrystalline hexamethylethane (taken from Chezeau *et al.* (1971)). T.P., M.P. and B.P. are the transition temperature to the plastic phase, the melting point and boiling point, respectively.

Calculations for close-packed molecular solids (Burton and Jura 1967) predict that, for a monovacancy diffusion mechanism, $V^* = 1{\cdot}2\Omega$, where Ω is the molecular volume. For the divacancy mechanism the same calculations yielded $V^* = 1{\cdot}8\Omega$. The value of Ω at 20°C for hexamethylethane is $137\,\mathrm{cm^3\,mol^{-1}}$, and therefore the NMR data are consistent with the monovacancy mechanism at low temperatures ($V^* = 1{\cdot}12\Omega$) with an increasing contribution from divacancies at higher temperatures ($V^* \cong 1{\cdot}6\Omega$). Thus the pressure data have helped to construct the model of self-diffusion in hexamethylethane.

In terms of the diffusion behaviour hexamethylethane is a well-behaved material and the NMR data are consistent with the results of radiotracer and creep measurements (Sherwood 1979 b). Unfortunately the picture is less clear for other plastic crystals. Briefly, the plastic crystals can be classified in terms of their entropy of

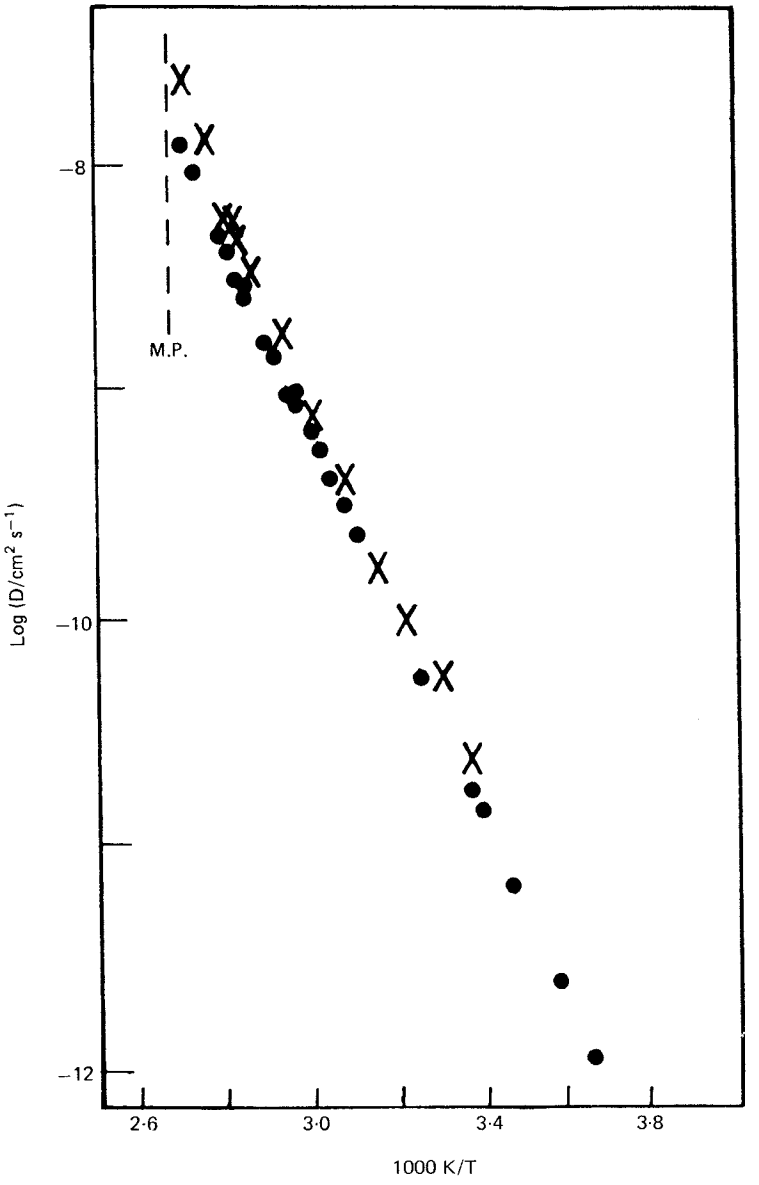

Figure 7. The diffusion coefficients for hexamethylethane plotted as a function of reciprocal temperature. The points marked are obtained from the NMR relaxation measurements using a Wolf analysis (Britcher and Strange 1979) and the points marked X are radiotracer measurements (Lockhart and Sherwood 1972).

fusion S_f. For high S_f materials ($S_f > 2k$) all the diffusion techniques are in agreement with each other and the simple theoretical predictions for a dominant monovacancy mechanism holds, as in hexamethylethane ($S_f = 2{\cdot}4k$). However, for low S_f materials ($S_f \sim 1k$), like cyclohexane ($S_f = 1k$), whilst radiotracer and creep experiments still yield $Q^* \sim 2L_s$ the NMR experiments yield typically $Q^* \sim 1L_s$. This discrepancy and the implications in terms of mechanisms and the interpretation of the NMR measurements has still to be fully resolved (Boden 1979).

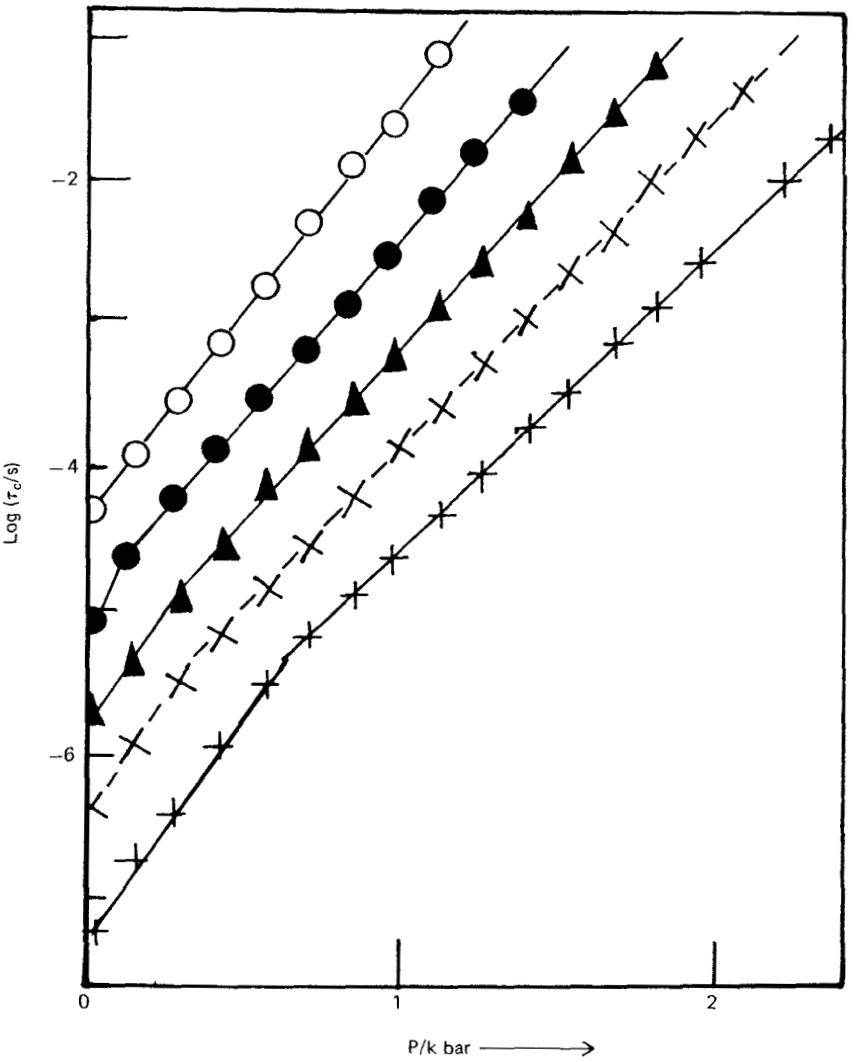

Figure 8. Isotherms for $\log \tau_c$ as a function of pressure in polycrystalline hexamethylethane. The data points were obtained by analysing T_ρ measurements on the basis of a Torrey model (after Ross and Strange (1978)) (○, 295·0 K; ●, 314·7 K; ▲, 329·3 K; X, 346·9 K; +, 368·0 K.

4.2. *Ionic crystals with the fluorite structure*

There has been considerable interest in the materials with the fluorite structure (Hayes 1974) and attention has recently been focused on the high temperature point defect and transport behaviour (Chadwick 1983, Hutchings *et al.* 1984, Gillan 1985, 1986 a, b, Allnatt *et al.* 1987). It is appropriate to outline some of the properties prior to a consideration of the NMR experiments. This will be restricted to the halides (CaF_2, SrF_2, BaF_2, β–PbF_2 and $SrCl_2$), although similar effects have been predicted in other materials possessing the fluorite structure.

In CaF_2 the anions form a simple cubic sub-lattice and alternate cubes are occupied by the divalent cations. At low to moderate temperatures the fluorites are normal ionic crystals (Lidiard 1974). The point defects are anion Frenkel pairs, i.e. anion vacancies and anions on the cube-centre interstitial sites, and all the experimental evidence points to the fact that atomic transport involves only these defects. Disorder and transport on the cation sub-lattice is negligible. An excess of interstitial anions can be introduced by doping with M^{3+} cations (e.g. La^{3+}) and excess anion vacancies by M^{+} (e.g. Na^{+} or K^{+}) or O^{2-} doping. At approximately 0·8 of the melting temperature (T_m), usually termed T_c, the fluorite structures exhibit a broad thermal anomaly in the specific heat curve which has the appearance of a λ-type order–disorder transition (Dworkin and Bredig 1968). In the same temperature regime as the onset of the thermal anomaly the ionic conductivity rises rapidly to values around 1 $ohm^{-1}\,cm^{-1}$ and then shows only a small increase beyond T_c. A typical conductivity plot is shown in figure 9. In the high temperature region the magnitude of the conductivity classes the fluorites as fast-ion

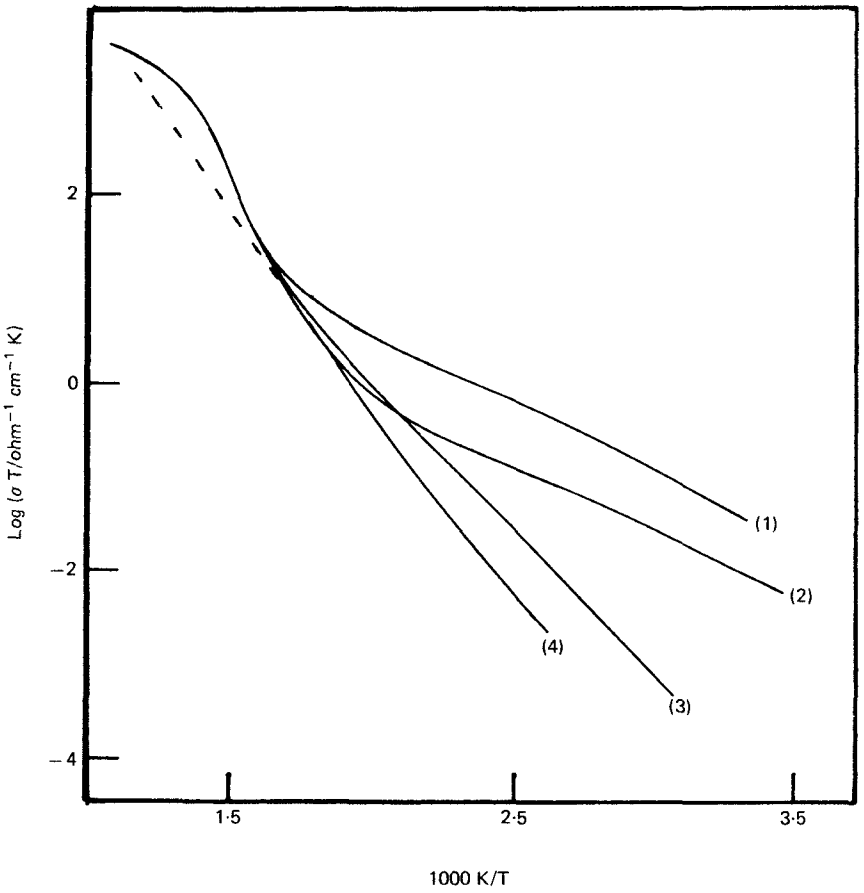

Figure 9. The plot of $\log \sigma T$ as a function of reciprocal temperature for β-PbF_2 single crystals. Nominal dopant levels (1) 1000 p.p.m. Na^{+}; (2) 100 p.p.m. Na^{+}; (3) 100 p.p.m. La^{3+}; (4) pure (after Azimi *et al.* (1964). These plots are typical of the halides with the fluorite structure. The dashed line is an extrapolation of the low temperature behaviour to emphasize the transition to the fast-ion region.

conductors, solid electrolytes or superionic conductors (Salamon 1979, Kleitz *et al.* 1983).

Since the fluorites are structurally the simplest of all fast-ion conductors they have been extensively studied as model systems. The earliest theoretical model of the fluorites proposed that the thermal anomaly represented the generation of massive concentrations of Frenkel defects to the extent that the anions randomly occupied the normal anion sites and the interstitial sites. This concept of a molten sub-lattice is clearly attractive as it would predict liquid-like diffusion of the anions and would explain the conductivity. We will see later that this model is not confirmed in mechanistic studies.

Ionic transport in the low temperature region of the fluorites, i.e. before the onset of fast-ion conductivity, has been extensively studied by NMR methods. Here we will concentrate on the work of Strange and his collaborators (which is summarized in Gordon and Strange (1979)) as their original approach was specifically to use these materials as test-beds of NMR methods of identifying diffusion mechanisms. In addition, these studies have made full use of the theoretical developments outlined in section 2.3. It will be recalled that the possible mechanisms that can give rise to transport in the fluorites are shown in figure 5. But which of these mechanisms is dominant and how do the interstitial anions migrate in deliberately M^{3+} doped crystals? These questions were answered by the combined measurements of NMR relaxation times and ionic conductivity on the same single crystal samples (Figueroa *et al.* 1978, Kirkwood 1980).

Consider first the data for pure BaF_2 crystals (Figueroa *et al.* 1978). The ^{19}F relaxation times T_1, T_2, $T_{1\rho}$ and T_{1D} were measured for these crystals and the results (some of which are shown in figure 10) led to diffusion coefficients being evaluated using the Wolf encounter model which takes account of the correlation effects (see § 3.2). By a coincidence the assumption of either a vacancy or an interstitialcy mechanism leads to virtually the same value of D_{NMR}, the difference being only 4%. However, the value of D_σ depends strongly on whether vacancy, $D_{\sigma v}$, or interstitialcy, $D_{\sigma i}$, is assumed since for anion diffusion in fluorites $D_{\sigma i} = \frac{3}{4} D_{\sigma v}$. This difference arises because of the differences in the scalar displacement caused by a vacancy and interstitialcy jump (Figueroa *et al.* 1978). Thus the Haven ratio type of approach is possible to distinguish between the two mechanisms. In figure 11 the values of D_{NMR} and $D_{\sigma v}$ are plotted and should coincide if the vacancy mechanism is operative. The differences, though very small and not easily distinguished (figure 11), are 18% at low temperatures and 8% at high temperatures, D_σ being smaller than D_{NMR}. Given the experimental error these results are support for a vacancy mechanism, as $D_{\sigma i}$ would be smaller than $D_{\sigma v}$. This is in agreement with theoretical predictions for the low temperature region. There is a distinct curvature in both $D_{\sigma v}$ and D_{NMR} at $T \sim 830$ K, which indicates the onset of another mechanism. In the analysis of conductivity data this is usually assumed to be the interstitialcy mechanism starting to make a significant contribution at the higher temperatures in fluorites (Azimi *et al.* 1984). Thus the high temperature region would be expected to be better fitted by assuming an interstitialcy process in analysing the NMR measurements, but this is not the case.

The general agreement between D_{NMR} and D_σ in figure 11 is impressive as it covers diffusion coefficients ranging over nine orders of magnitude. Thus the comparative test of the two techniques is very severe and is rather unique in transport studies.

The above experiments on pure BaF_2 crystals were also performed on O^{2-}, K^+ and La^{3+} doped single crystals of BaF_2 (Figueroa *et al.* 1978). The results for the two

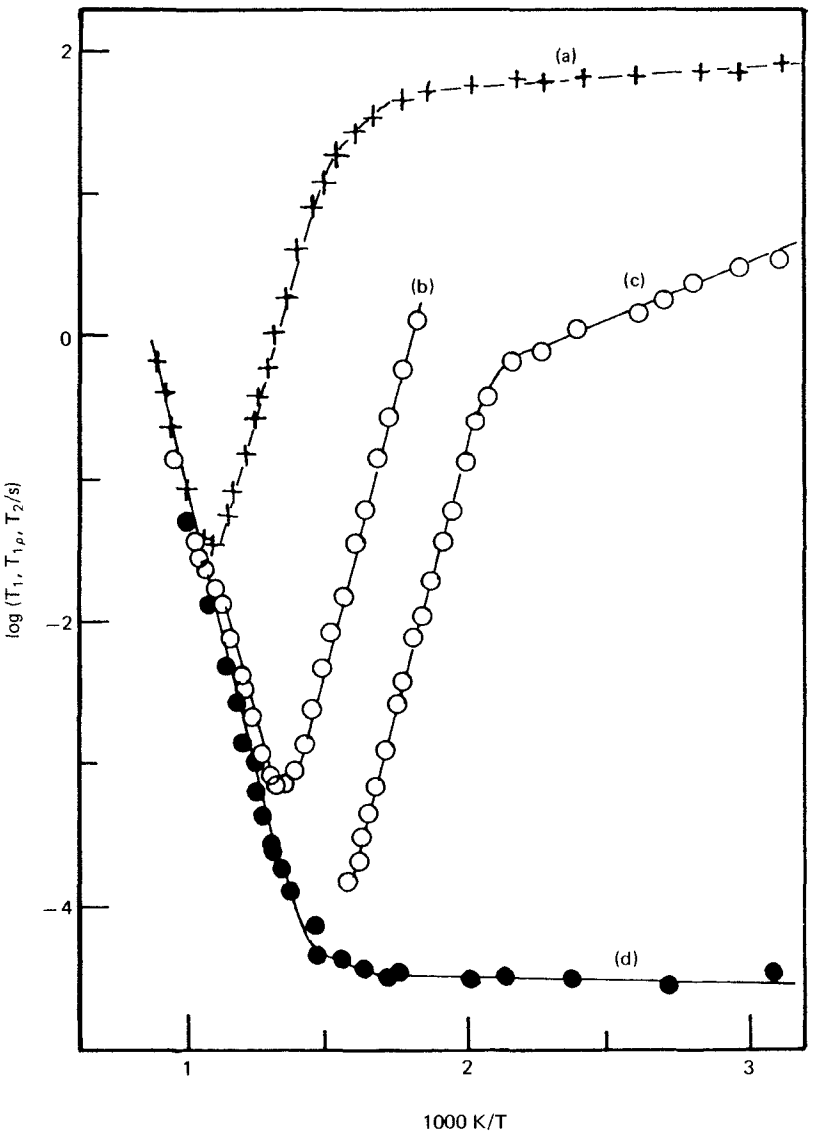

Figure 10. The temperature dependence of the ^{19}F relaxation times in pure BaF_2 single crystals: (*a*) T_1 ($\mathbf{B}_0//\langle 110\rangle$); (*b*) $T_{1\rho}$ at $B_1 = 12$ G ($\mathbf{B}_0//\langle 110\rangle$); (*c*) T_{1D} ($\mathbf{B}_0//\langle 110\rangle$); (*d*) T_2 ($\mathbf{B}_0//\langle 100\rangle$) (After Figueroa *et al.* (1978)).

cation-doped crystals are shown in figure 12, where D_{NMR} is compared with $D_{\sigma v}$. For the low temperature (extrinsic) region of the K^+ doped crystal the agreement between D_{NMR} and $D_{\sigma v}$ is excellent, differences being only a few per cent. This is to be expected since in this temperature regime the only mobile defects are the anion vacancies. The experiment on O^{2-} doped crystal also confirmed the expected vacancy mechanism. There is a departure between D_{NMR} and $D_{\sigma v}$ for the K^+ doped crystal at the lowest temperatures which is due to the effects of association (Lidiard 1974). There is an attraction between the K^+ ion and the anion vacancy due to their opposite virtual

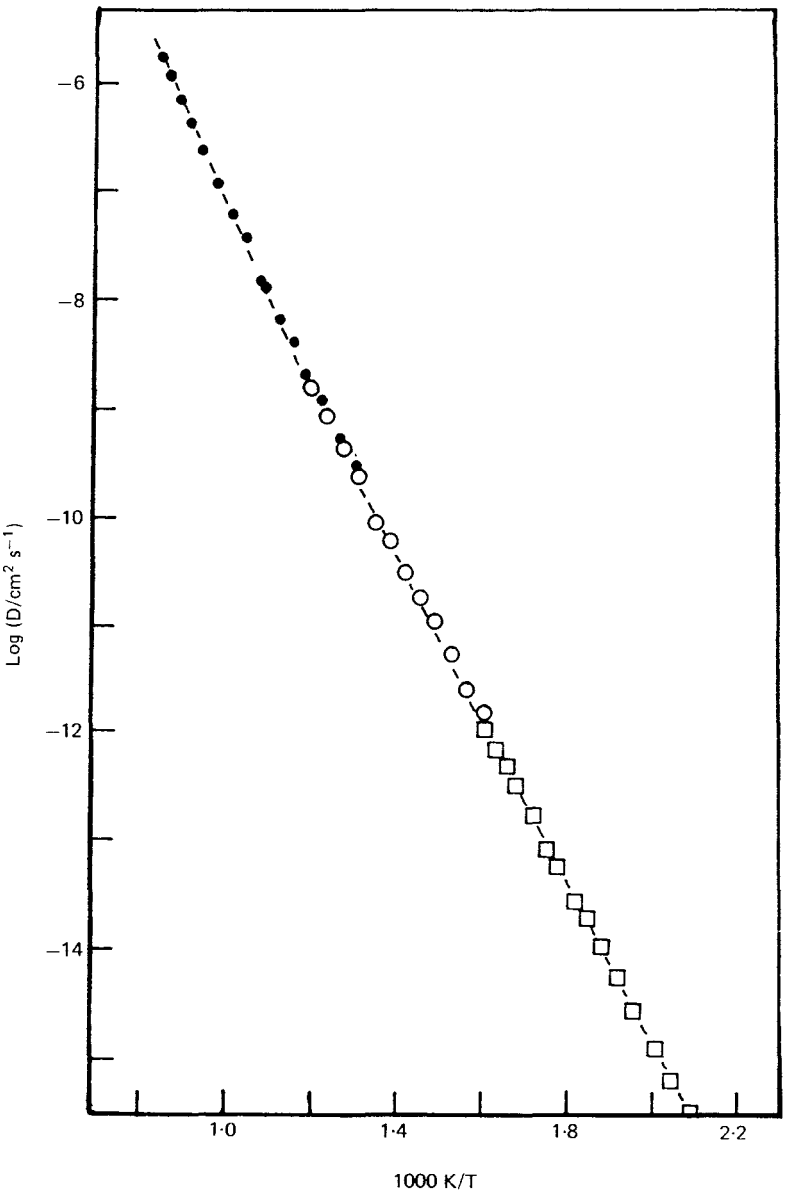

Figure 11. The temperature dependence of the fluorine self-diffusion coefficients in pure BaF_2 single crystals evaluated from: (*a*) conductivity ($D_{\sigma v}$) (– – – –); (*b*) NMR; ● T_1, ○ $T_{1\rho}$, □ T_{1D} (after Figueroa *et al.* (1968)).

charges and this will result in the two forming nearest-neighbour complexes at low temperatures. These 'bound' vacancies will not be able to contribute to the ionic conductivity and this results in the downward curvature of $\log D_{\sigma v}$ as $1000\,K/T$ increases (T decreases) seen in figure 12. However, the bound vacancies will undergo local motion around the K^+ ion and this motion will contribute to the NMR relaxation processes.

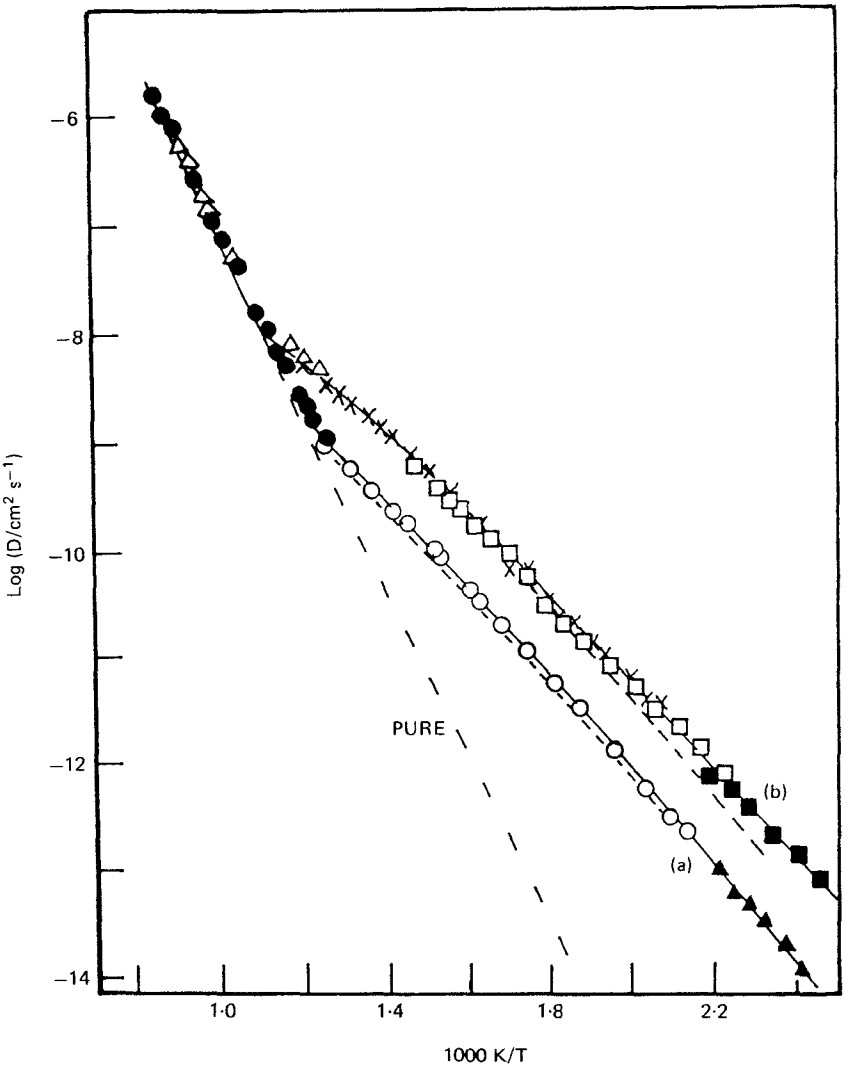

Figure 12. The temperature dependence of the fluorine self-diffusion coefficients in BaF_2 crystals containing cation impurities: (*a*) 0·050% LaF_3 doped BaF_2; (– – – –) $D_{\sigma v}$; NMR; ● T_1, ○ $T_{1\rho}$, ▲ T_{1D}. (*b*) 0·040% KF doped BaF_2; (– – – –) $D_{\sigma v}$; NMR; △ T_1, □ and X $T_{1\rho}$, ■ T_{1D} (after Figueroa *et al.* (1968)).

In the extrinsic region of La^{3+}-doped BaF_2 there are excess interstitial anions and the diffusion is expected to proceed via the interstitialcy mechanism. However, a better fit to the data was obtained by assuming a vacancy mechanism. The difference between $D_{\sigma v}$ and D_{NMR} is about 16% and it is $D_{\sigma v}$ that is drawn in figure 12. If interstitialcy diffusion is assumed then the difference between $D_{\sigma i}$ and D_{NMR} is about 40%. Thus the expected interstitialcy mechanism was not confirmed in the extrinsic region of this crystal.

The lack of any evidence from this work for interstitialcy diffusion in BaF_2 crystals, particularly in the La^{3+} doped crystals, was the cause of some concern (Figueroa *et al.* 1978). It was not due to any obvious factor in the theoretical interpretation and the

authors suggested that the experiments be repeated for another system. This was pursued with La^{3+} doped SrF_2 (Kirkwood 1980) and the expected interstitialcy mechanism was verified in this system. Thus the La^{3+} doped BaF_2 experiments should be repeated.

It is worth noting that the activation energies obtained from NMR methods for the fluorites are in good agreement with the activation energies from conductivity (Chadwick 1983), and that the NMR values agree well with calculated energies of defects based on the static lattice model (Catlow *et al.* 1977). This provides useful, but indirect confirmation of the mechanisms.

Attempts (Wolf *et al.* 1977, Figueroa *et al.* 1979) to use solely the NMR relaxation-time measurements for BaF_2 crystals to identify the diffusion mechanisms have not been successful. In principle, identification should be possible from the temperature dependence (Figueroa *et al.* 1979) and the orientation dependence (Wolf *et al.* 1977) of the relaxation times. However, in all the crystals investigated, and at all temperatures, the predicted differences between vacancy and interstitialcy diffusion were too small to be detected with the available experimental precision. Nevertheless, this work was significant as the results supported the Wolf model and showed the inappropriateness of the random-walk models in detailed interpretations of NMR measurements in solids.

In the fast-ion conduction region of the fluorites it has been possible to employ NMR methods to test the concept of the molten sub-lattice. If the motion of the anions is indeed liquid-like, then the diffusion would be highly-correlated and solid-state models would be inappropriate in the evaluation of D_{NMR}. The prediction would be that $D_{NMR} \ll D_\sigma$ and the combination of NMR and conductivity experiments described above for BaF_2 would provide the test-bed.

The most appropriate system for this test is β-PbF_2, for which T_c is only 711 K. The ^{19}F relaxation times T_1, $T_{1\rho}$ and T_2 were measured by Boyce *et al.* (177) and the evaluated diffusion parameters compared with literature conductivity data. They found that at low temperatures D_{NMR}/D_σ was approximately unity but decreased in the fast-ion region to about 0·1, suggesting highly correlated anion motion. However, their relaxation times in the fast-ion region showed unusual behaviour; T_2 was not equal to T_1 (cf. figure 4). Later work (Hogg *et al.* 1977) demonstrated that, in the fast-ion region, small amounts of paramagnetic impurity (as low as 1 p.p.m.) could give rise to the effects observed by Boyce *et al.*, and that these were not necessarily due to highly correlated diffusion. Gordon and Strange (1978) repeated the NMR measurements and found results similar to those of Boyce *et al.* in the fast-ion region. However, they found that the results were not reproducible on thermal cycling and that heating β-PbF_2 in a silica tube gave rise to an appreciable ESR signal. This was believed to result from reaction between the sample and silica, oxygen or water vapour. All the fluorides are highly reactive at high temperatures; hence relaxation time measurements are inappropriate for studying diffusion in the fast-ion region.

Gordon and Strange (1978) used the p.f.g. method to measure ^{19}F diffusion in β-PbF_2 single crystals. These measurements, being less susceptible to the effect of paramagnetic impurities, gave reliable values of D, which is effectively D_{tracer}. However, when combined with literature conductivity data this gave $D/D_\sigma = H_R \sim 0{\cdot}3$ in the fast-ion region. The conductivity was re-measured (Carr *et al.* 1978) using the same source of single crystals as Gordon and Strange (see figure 13). The value of H_R was now between 0·7 and 1·0, which is consistent with the values found in lowly defective, normal ionic crystals. These results therefore demonstrate the failure of the molten sub-lattice

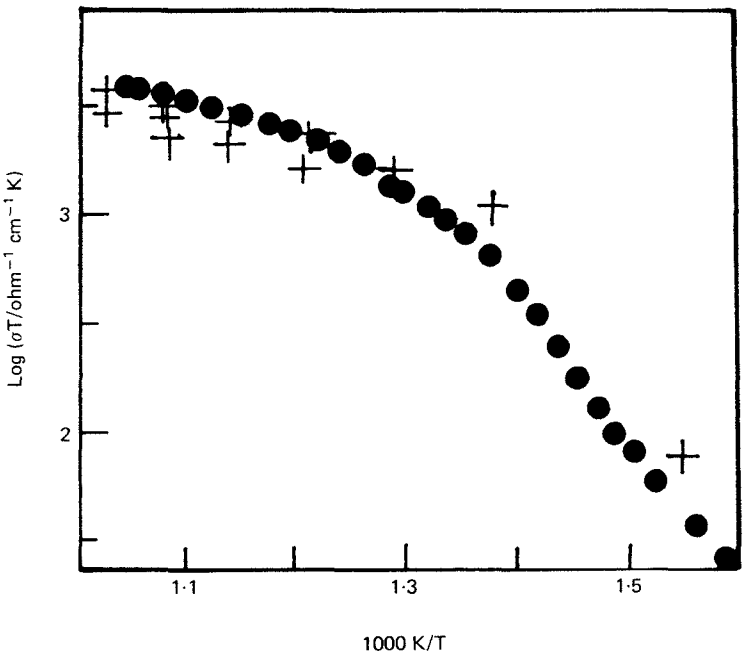

Figure 13. The temperature dependence of the conductivity of β-PbF_2 in the fast-ion regime: ●, conductivity measurements; +, conductivity calculated from the p.f.g.-NMR data assuming a vacancy mechanism (after Carr *et al.* (1978)).

concept and indicate the conduction involves the migration of a small number ($\sim 2\%$) of mobile defects.

The determination of the exact nature of the structure and transport in the fast-ion region of fluorites is extremely difficult. Neutron scattering data, reviewed by Hutchings *et al.* (1984), suggests that a large fraction (around 45%) of the anions have moved off their normal lattice sites, although the number of true defects was much smaller. Coherent diffuse quasi-elastic neutron scattering (QES) provided evidence for short-lived defect clusters and several cluster models were proposed to explain the neutron data. Computer simulations (Allnatt *et al.* 1987) showed that certain cluster structures were particularly stable and defect clustering would explain the onset of the fast-ion region. This would be consistent with the NMR data as the clusters would not be mobile and the concentration of 'free' defects would be small. However, it should be mentioned that Gillan (1985, 1986 a, b) has offered an alternative explanation of the QES data and ascribed it to defect motion without the need to invoke clusters. This was based on molecular dynamics simulations which quantitatively reproduced the neutron experiments.

4.3. *Polyether electrolytes*

The complexes formed by alkali metal salts (MX) and high molecular weight polyethylene oxide (PEO) are good ionic conductors at elevated temperatures (Wright 1975, Armand *et al.* 1979), as can be seen from a typical conductivity plot shown in figure 14. These materials can be formed as thin, flexible films and became the focus of intense interest following their proposed application as the electrolytes in solid state

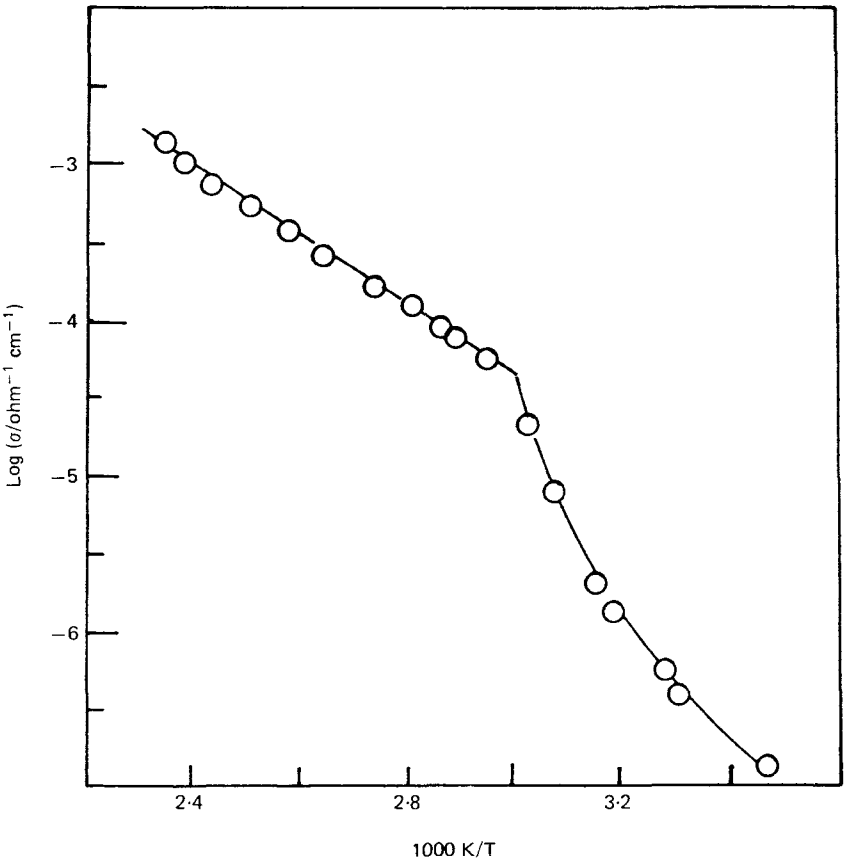

Figure 14. The plot of log σ as a function of reciprocal temperature for NaSCN.PEO_8 (after Chadwick *et al.* (1983)).

batteries (Armand *et al.* 1979). Recent work has shown that a wide range of polymers containing ethoxy units, either in the backbone or side-chain, will form conducting films when doped with salts (Cowie 1987, Vincent 1987, Ratner and Shriver 1988). This general class of ionically conducting materials is referred to as polymer electrolytes and they are still a centre of research activity, particularly for lithium batteries. The most extensively investigated materials remain those based on PEO and they are model systems. NMR techniques have played a major role in understanding both the structure and transport in polyether electrolytes, and some of the work is described below.

As expected the cations in these electrolytes are coordinated to the oxygen atoms of the polyether chain and this has been demonstrated by EXAFS (Catlow *et al.* 1983). From simple analogies with crown ether complexes of salts it was generally assumed there were four ether oxygens coordinated to the cation and the fully stoichiometric compound was designated MX.PEO_4. However, materials are known with three-fold ether oxygen coordination and the composition of the stoichiometric material depends on the nature of the salt. Optimum conductivity is found in materials containing excess PEO, i.e. compositions around MX.PEO_{10}. These materials have complex phase diagrams and a problem was to relate the morphology to the conductivity. At low

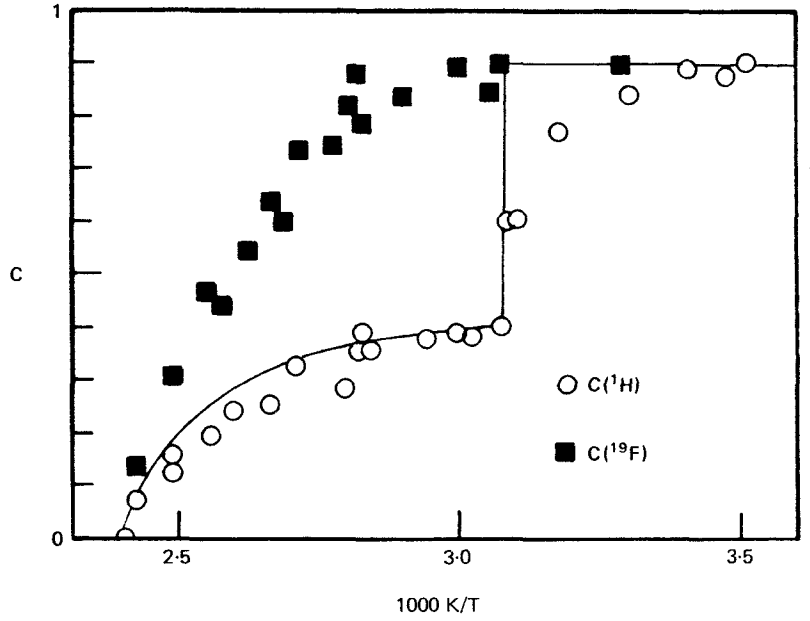

Figure 15. The fraction of protons, $C(^1H)$, and fluorine, $C(^{19}F)$, in the crystalline phase of $LiCF_3SO_3.PEO_8$. The solid line represents calorimetric data (after Minier *et al.* (1984)).

temperatures, below the melting point of pure PEO (~ 338 K), there are two dominant phases, crystalline stoichiometric complex and crystalline PEO plus a small fraction of amorphous PEO. Above the melting point of PEO the system contains elastomeric or liquid PEO and crystalline complex. As the temperature increases the complex dissolves into the elastomeric phase until, at some temperature, complete dissolution occurs. This picture was confirmed in an elegant study of $LiCF_3SO_3.PEO_8$ by Minier *et al.* (1984) who combined ^1H and ^{19}F NMR measurements (FID determined by spin-echo) with calorimetric measurements. Nuclei in crystalline and elastomeric phases have very different values of T_2. Thus it was possible to monitor the fractions of protons and fluorine atoms (the $CF_3SO_3^-$ ions) in the crystalline phase as a function of temperature. The data are shown in figure 15. The NMR data correlated well with the calorimetric data and proved that the conductivity was due to ions moving in the elastomeric phase. As a result the synthetic goal of an ambient temperature polymer electrolyte must meet the criterion that the material is elastomeric.

There have been many attempts to use NMR methods to monitor the diffusion of ions in polyether electrolytes (Chadwick and Worboys 1987). There are often problems in relating the measured line-width and relaxation time in polyether electrolytes with the ionic motion for a variety of reasons; the complexity of the morphology, the use of nuclei with quadrupole moments, etc. It is also important to study both ions of the salt as radiotracer work has shown that Na^+ and SCN^- have comparable mobilities in $NaSCN.PEO_8$, the anion being the more mobile (Chadwick *et al.* 1983). The diffusion in the elastometer phase is fast enough to employ the p.f.g.-NMR technique and this is proving a very powerful tool in these systems, particularly as Li^+ diffusion coefficients can be measured, which is important for battery technology. Some of the available p.f.g.-NMR diffusion data in PEO electrolytes are shown in figure 16. These show that in $LiCF_3SO_3PEO_8$ the anions are the more mobile species. In principle, the diffusion

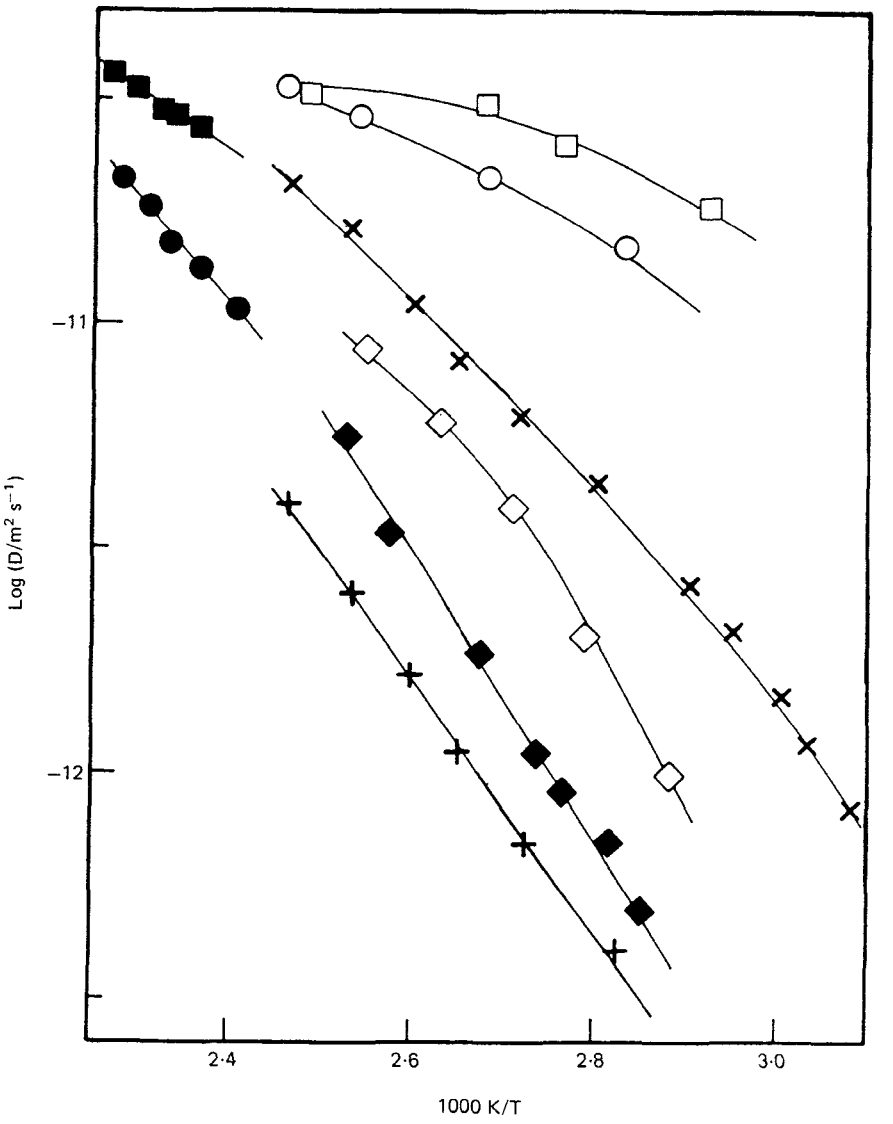

Figure 16. The p.f.g.-NMR diffusion data for LiX.PEO_x polyether electrolytes, ●, ^{7}Li and ■, ^{19}F in $LiCF_3SO_3.PEO_8$ (after Battacharja *et al.* (1986)); ○, ^{7}Li and □, ^{19}F in $LiCF_3SO_3.PEO_8$ (after Mali *et al.* (1984)); ×, ◆ and +, ^{7}Li in $LiClO_4.PEO_x$, where $x=6$, 8 and 20 (after Gorecki *et al.* (1986)). ◇, ^{19}F in $LiClO_4.PEO_8$ (after Mali *et al.* (1984)).

coefficients obtained from p.f.g.-NMR could be compared with the conductivity and the Haven ratio used to provide information on the migration processes. However, great care is necessary as the samples may not be fully amorphous and a good phase diagram is required to calculate the precise fraction of elastomeric phase and the concentration of mobile ions. There is some debate concerning the value of H_R (Ratner and Shriver 1988). Qualitatively, the ions migrate via the segmental motion of the polymer; however, the role of ion–ion interactions and ion aggregation on the transport has to be resolved. Accurate p.f.g.-NMR diffusion coefficients have a part to play in attacking these problems.

5. Summary

NMR methods serve as powerful probes for the elucidation of mechanisms of diffusion within solids. A rather restricted number of systems was included and particular attention was deliberately given to the work on the fluorites as it was important in setting a firm foundation to the procedures, both experimental and theoretical, especially the verification of the Wolf model. Other particularly noteworthy examples not discussed here are some of the studies of fast-ion conductors (e.g. Li_3N, where NMR has shown the existence of interlayer diffusion (Brinkmann 1983)). There are still some details that have to be resolved and the discrepancies between the NMR and radiotracer diffusion activation energies in some of the plastic solids remain contentious. These may be a feature of the materials under investigation and be related to the rotational disorder or the dislocation structure (Sherwood 1979 b). NMR methods also have their limitations. Problems associated with paramagnetic impurities, sensitivity to dilute spin concentrations, and sample inhomogeneity are but a few that are discussed here. Other problems arise in studies of solids at elevated temperatures—the intensity of the resonance signal decreases exponentially with increasing temperature, and special furnace designs are required to heat samples in the confined space between the magnet poles. In addition, detailed studies, like those described for the fluorites, require large ($\sim 1\ cm^3$) single crystals. Similarly, Wolf has fully developed his encounter model only for the b.c.c. and f.c.c. lattices, although, in principle, it could be extended to other structures. However, this level of information is not always required and the usefulness of the NMR techniques depends on the particular material and the problem under consideration. For example, activation energies are quickly and reliably obtained and this may be sufficient to give a strong indication of the mechanism. Similarly, mechanisms can often be deduced from the structural information provided by NMR spectroscopy.

Finally, a few comments on future developments are appropriate. Specifically, some of the procedures used in the work described in this review could be improved in future investigations. A major problem in the work on the fluorites and polyether electrolytes is maintaining a high degree of precision in both the conductivity and NMR experiments. Difficulties such as the regular but tedious cross-calibration of thermocouples arise due to the two experiments being performed separately. A novel approach is to conduct the conductivity measurement, or another type of transport measurement, simultaneously with the NMR measurement leading to a greater reliability and precision. Such work is currently in progress in our laboratory. On the general level some of the techniques described here will find a wider application, and the increasing availability of spectrometers with high-field magnets will inevitably widen the range of materials that can be investigated. Recently, the self-diffusion of ^{17}O in doped ceria was measured by NMR methods (Fuda *et al.* 1984), showing their exciting potential for the study of transport in oxides. The p.f.g.-NMR method of measuring diffusion coefficients directly, initially so successfully applied to the study of β-PbF_2, and latterly with polyether electrolytes, seems an ideal probe for the investigation of fast-ion conductors. The high-resolution spectra for solids that can be obtained by using cross-polarization and magic-angle spinning techniques will provide very valuable structural information on which to build diffusion models. An obvious example where this would be useful is with the polyether electrolytes. Overall there seems to be a bright future for NMR in probing the mechanisms of solid-state diffusion.

Acknowledgments

I am deeply indebted to Professor J. H. Strange, my colleague and collaborator for many years. His constructive comments and general advice were extremely important in the preparation of this article. I am also very grateful to Professor J. M. Thomas for suggestions which have improved the review.

References

ABRAGAM, A., 1961, *The Principles of Nuclear Magnetism* (London: Oxford University Press).
ADDA, Y., and PHILIBERT, J., 1966, *La diffusion dans les solides* (Paris: Dunod).
ALLEN, P. S., 1972, *MTP International Review of Science—Physical Chemistry Series One*, Volume 4, edited by A. D. Buckingham (London: Butterworth), p. 43.
AILION, D. C., 1971, *Adv. magn. Res.*, **5**, 177.
AILION, D. C., and HO, P. P., 1968, *Phys. Rev.*, **168**, 662.
AKITT, J. W., 1982, *NMR and Chemistry: an Introduction to the Fourier Transform-Multinuclear Era* (London: Chapman and Hall).
ALBERT, S., GUTOWSKY, H. S., and RIPMEESTER, J. A., 1972, *J. Chem. Phys.*, **56**, 1332.
ALLNATT, A. R., CHADWICK, A. V., and JACOBS, P. W..M., 1987, *Proc. Roy. Soc., London*, **A410**, 385.
ANDREW, E. R., 1981, *Int. Rev. Phys. Chem.*, **1**, 195.
ARMAND, M. B., CHABAGNO, J. M., and DUCLOT, N. J., 1979, in *Fast Ion Transport in Solids*, edited by P. Vashishta, J. N. Mundy and G. K. Shenoy (Amsterdam: North Holland), p. 131.
AZIMI, A., CARR, V. M., CHADWICK, A. V., KIRKWOOD, F. G., and SAGHAFIAN, R., 1984, *J. Phys. Chem. Solids*, **45**, 23.
BHATTACHARJA, S., SMOOT, S. W., and WHITMORE, D. H., 1986, *Solid State Ionics*, **18/19**, 306.
BLOEMBERGEN, N., PURCELL, E. M., and POUND, R. V., 1948, *Phys. Rev.*, **73**, 679.
BODEN, N., 1979, in *The Plastically Crystalline State*, edited by J. N. Sherwood (New York: Wiley), pp. 147–214.
BOYCE, J. B., MIKKELSEN, J. C., and O'KEEFFE, M., 1977, *Solid State Commun.*, **21**, 955.
BRINKMANN, D., 1983, in *Progress in Solid Electrolytes*, edited by T. A. Wheat, A. Ahmad and A. K. Kuriakose (Ottawa: Canmet), pp. 1–26.
BRITCHER, A. R., and STRANGE, J. H., 1979, *Molec. Phys.*, **37**, 181.
BURTON, J. J., and JURA, G., 1967, *J. Phys. Chem. Solids*, **28**, 705.
CARR, V. M., CHADWICK, A. V., and SAGHAFIAN, R., 1978, *J. Phys. C*, **11**, L637.
CATLOW, C. R. A., CHADWICK, A. V., GREAVES, G. N., MORONEY, L. M., and WORBOYS, M. R., 1983, *Solid State Ionics*, **9** and **10**, 1107.
CATLOW, C. R. A., and MACKRODT, W. C., 1982, *Computer Simulation of Solids* (Heidelberg: Springer).
CATLOW, C. R. A., NORGETT, M. J., and ROSS, T. A., 1977, *J. Phys. C*, **10**, 1627.
CHADWICK, A. V., 1983, *Solid State Ionics*, **8**, 209.
CHADWICK, A. V., FORREST, J. W., GRIMWOOD, A. A., and STRANGE, J. H., 1976, *Molec. Phys.*, **32**, 1773.
CHADWICK, A. V., and GLYDE, H. R., 1977, in *Rare Gas Solids*, Vol. II, edited by M. L. Klein and J. A. Venables (New York: Academic Press), p. 1151.
CHADWICK, A. V., WORBOYS, M. R., and STRANGE, J. H., 1983, *Solid State Ionics*, **9** and **10**, 1155.
CHADWICK, A. V., and WORBOYS, M. R., 1987, in *Polymer Electrolyte Reviews*—1, edited by J. R. MacCallum and C. A. Vincent (London: Elsevier), p. 275.
CHEZEAU, J. M., DUFOURCQ, J., and STRANGE, J. H., 1971, *Molec. Phys.*, **20**, 305.
CHEZEAU, J. M., and STRANGE, J. H., 1979, *Phys. Rep.*, **53**, 1.
COMPAAN, K., and HAVEN, Y., 1958, *Trans. Faraday Soc.*, **54**, 1498.
CORISH, J., and JACOBS, P. W. M., 1973, in *Surface and Defect Properties of Solids*, Vol. II, edited by M. W. Roberts and J. M. Thomas (London: Chemical Society), Chap. 7.
COWIE, J. M. G., 1987, in *Polymer Electrolyte Reviews*—1, edited by J. R. MacCallum and C. A. Vincent (London: Elsevier), p. 69.

DWORKIN, A. S., and BREDIG, M. A., 1968, *J. chem. Phys.*, **72,** 1277.
EISENSTADT, M., and REDFIELD, A. G., 1963, *Phys. Rev.*, **132,** 635.
FARRAR, T. C., and BECKER, E. D., 1971, *Pulse and Fourier Transform NMR* (New York: Academic Press).
FIGUEROA, D. R., CHADWICK, A. V., and STRANGE, J. H., 1978, *J. Phys. C*, **11,** 55.
FIGUEROA, D. R., STRANGE, J. H., and WOLF, D., 1979, *Phys. Rev.* B, **19,** 148.
FUDA, K., KISHIO, K., YAMAUCHI, S., FUEKI, K., and ONODA, Y., 1984, *J. Phys. Chem. Solids*, **45,** 1253.
FYFE, C. A., THOMAS, J. M., KLINOWSKI, J., and GOBBI, G. C., 1983, *Angew. Chem. Edb* **22,** 259.
GILLAN, M. J., 1985, *Physica*, **131B,** 157.
GILLAN, M. J., 1986 a, *J. Phys. C*, **19,** 3391.
GILLAN, M. J., 1986 b, *J. Phys. C*, **19,** 3517.
GOLDMAN, M., 1970, *Spin Temperature and Nuclear Magnetic Resonance in Solids* (London: Oxford University Press).
GORDON, R. E., and STRANGE, J. H., 1978, *J. Phys. C*, **11,** 3213.
GORDON, R. E., and STRANGE, J. H., 1979, *Faraday Symp. Chem. Soc.*, **13,** 154.
GORDON, R. E., STRANGE, J. H., and WEBBER, J. B. W., 1978, *J. Phys. E*, **11,** 1051.
GORECKI, W., ANDREANI, R., BERTHIER, C., ARMAND, M. B., MALI, M., ROOS, J., and BRINKMANN, D., 1986, *Solid State Ionics*, **18/19,** 295.
GROSS, B., and KOSFELD, R., 1969, *Tagung Hoch-frequenziespecktroscopie* (Leipzig: Karl-Marx Universität), p. 352.
HARRIS, R. K., 1983, *Nuclear Magnetic Resonance Spectroscopy: A Physiochemical View* (London: Pitman).
HAYES, W., 1974, *Crystals with the Fluorite Structure* (Oxford: Clarendon Press).
HOGG, R. D., VERNON, S. P., and JACCARINO, V., 1977, *Phys. Rev. Lett.*, **39,** 481.
HOODLESS, I. M., STRANGE, J. H., and WYLDE, L. E., 1971, *J. Phys. C*, **4,** 2742.
HOODLESS, I. M., STRANGE, J. H., and WYLDE, L. E., 1973, *J. Phys., Paris*, **34,** C9–21.
HOWARD, R. E., and LIDIARD, A. B., 1964, *Rep. Prog. Phys.*, **27,** 261.
HUTCHINGS, M. T., CLAUSEN, K., DICKENS, M. H., HAYES, W., KJEMS, J. K., SCHNABEL, P. G., and SMITH, C., 1984, *J. Phys. C*, **17,** 3903.
JOST, W., 1960, *Diffusion* (New York: Academic Press), p. 116.
KIRKWOOD, F. G., 1980, Ph.D. thesis, University of Kent.
KLEITZ, M., SAPOVAL, B., and RAVINE, D., 1983, *Solid State Ionics*—83, Proceedings of the 4th International Conference on Solid State Ionics, Grenoble (France) 1983. Published as *Solid State Ionics* **9** and **10**.
KLINOWSKI, J., 1984, *Prog. NMR Spectroscopy*, **16,** 237.
KUBO, R., and TOMITA, K., 1954, *Proc. Phys. Soc. Japan*, **9,** 888.
LECLAIRE, A. D., 1970, in *Physical Chemistry; An Advanced Treatise*, Vol. 10, edited by H. Eyring, D. Henderson and W. Jost (New York: Academic Press), p. 261.
LIDIARD, A. B., 1974, in *Crystals with the Fluorite Structure*, edited by W. Hayes (Oxford: Clarendon Press), p. 101.
LIPPMAA, E., MAGI, M., SAMOSON, A., TARMAK, M., and ENGELHARDT, G., 1981, *J. Am. Chem. Soc.*, **103,** 4992.
LOCKHART, N. C., and SHERWOOD, J. N., 1972, *Faraday Symp. Chem. Soc.*, **6,** 57.
LOOK, D. C., and LOWE, I. J., 1966, *J. chem. Phys.*, **44,** 2995.
LUCKHURST, G. R., and GRAY, G. W., 1979, *The Molecular Physics of Liquid Crystals* (New York: Academic Press).
MALI, M., ROOS, J., and BRINKMANN, D., 1984, *Proc. XXII Congress Ampère*, Zurich, 1984, edited by K. A. Muller, R. Kirid and J. Roos (University of Zurich).
MEHRER, H., and SEEGER, A., 1972, *Cryst. Lattice Defects*, **3,** 1.
MINIER, M., BERTHIER, C., and GORECKI, W., 1984, *J. Phys., Paris*, **45,** 739.
NOACK, F., 1971, *NMR Basic Principles and Progress*, **3,** 83.
POWLES, J. G., 1959, *Rep. Prog. Phys.*, **22,** 433.
RATNER, M. A., and SHRIVER, D. F., 1988, *Chem. Rev.*, **88,** 109.
RESING, H. A., and TORREY, H. C., 1963, *Phys. Rev.*, **131,** 1102.
RICHARDS, P. M., 1979, in *Physics of Superionic Conductors*, edited by M. B. Salamon (Berlin: Springer), pp. 141–174.
ROSS, S. M., and STRANGE, J. H., 1978, *J. chem. Phys.*, **68,** 3078.

SALAMON, M. B., 1979, *Physics of Superionic Conductors* (Berlin: Springer).
SHERWOOD, J. N., 1973, in *Surface and Defect Properties of Solids*, Vol. II, edited by M. W. Roberts and J. M. Thomas (London: Chemical Society), Chap. 3.
SHERWOOD, J. N., 1979 a, *The Plastically Crystalline State* (New York: Wiley).
SHERWOOD, J. N., 1979 b, in *The Plastically Crystalline State*, edited by J. N. Sherwood (New York: Wiley), pp. 39–83.
SHEWMON, P. G., 1963, *Diffusion in Solids* (New York: McGraw-Hill).
SHOLL, C. A., 1974, *J. Phys. C*, **7**, 3378.
SHOLL, C. A., 1975, *J. Phys. C*, **8**, 1737.
SLICHTER, C. P., 1973, *The Principles of Magnetic Resonance* (New York: Harper and Row).
STEJSKAL, E. O., and TANNER, J. E., 1965, *J. Chem. Phys.*, **42**, 288.
THOMAS, J. M., and KLINOWSKI, J., 1985, *Adv. Catal.*, **33**, 199.
TORREY, H. C., 1953, *Phys. Rev.*, **92**, 962.
TORREY, H. C., 1954, *Phys. Rev.*, **96**, 690.
VINCENT, C. A., 1987, *Prog. solid state Chem.*, **17**, 145.
WHITTINGHAM, M. S., and SILBERNAGEL, B. G., 1977, in *Solid Electrolytes*, edited by P. Hagenmuller and W. van Gool (New York: Academic Press), pp. 93–107.
WOLF, D., 1974 a, *Phys. Rev.* B, **10**, 2710.
WOLF, D., 1974 b, *Phys. Rev.* B, **10**, 2724.
WOLF, D., 1975 a, *J. magn. Res.*, **17**, 1.
WOLF, D., 1975 b, *Proc. 18th Ampère Congress* (Nottingham University Press), p. 251.
WOLF, D., 1979, *Spin Temperature and Nuclear Magnetic Relaxation in Matter* (Oxford: Clarendon Press).
WOLF, D., FIGUEROA, D. R., and STRANGE, J. H., 1977, *Phys. Rev.* B, **15**, 2545.
WRIGHT, P. V., 1975, *Br. Polymer J.*, **7**, 319.